Inorganic Chemistry

Article

pubs.acs.org/IC

Broad-Band N^N Pt(II) Bisacetylide Visible Light Harvesting Complex with Heteroleptic Bodipy Acetylide Ligands

Fangfang Zhong,[†] Ahmet Karatay,[‡] Liang Zhao,[†] Jianzhang Zhao,*[,†] Cheng He,[†] Caishun Zhang,[†] Halime Gul Yaglioglu,[‡] Ayhan Elmali,[‡] Betül Küçüköz,[‡] and Mustafa Hayvali*[,§]

[†]State Key Laboratory of Fine Chemicals, School of Chemical Engineering, Dalian University of Technology, E-208 West Campus, 2 Ling Gong Road, Dalian 116024, People's Republic of China

[‡]Department of Engineering Physics, Faculty of Engineering and [§]Department of Chemistry, Faculty of Science, Ankara University, 06100 Beşevler, Ankara, Turkey

Supporting Information

ABSTRACT: Pt(II) dbbpy bisacetylide (dbbpy = 4,4′-di(*tert*-butyl)-2,2′-bipyridine) complex (**Pt-1**) with two different Bodipy ligands was prepared with the goal to attain broad-band visible light absorbing, efficient funneling of the photoexcitation energy (via resonance energy transfer, RET) to the energy acceptor and high triplet formation quantum yields. Construction of the above-mentioned molecular structural motif is challenging because two different arylacetylide ligands are incorporated in the complex; normally two homoleptic acetylide ligands were used for this kind of N^N Pt(II) complexes. A reference complex with trans bis(tributylphosphine) Pt(II) bisacetylide protocol (**Pt-4**) was prepared for comparison of the photophysical properties. The two different Bodipy ligands in **Pt-1** and **Pt-4** constitute singlet/triplet energy donor/acceptor, as a result the harvested photoexcitation energy can be funneled to the triplet state confined on one of the two Bodipy ligands. The photophysical properties of the complexes were studied with steady state UV−vis absorption and luminescence spectroscopies, femto- and nanosecond transient absorption spectroscopies, cyclic voltammetry, as well as DFT/TDDFT calculations. Fluorescence/phosphorescence dual emission were observed for the complex. The ultrafast intramolecular singlet/triplet energy transfer in **Pt-1** was confirmed by the transient absorption spectroscopy (k_{FRET} = 2.6 × 10^{11} s^{-1}, Φ_{FRET} = 87.1%) followed by an intersystem crossing (k_{ISC} = 1.9 × 10^{10} s^{-1}), and the triplet state lifetime (τ_T) is 54.1 μs. The reference complex **Pt-4** shows drastically different kinetics with k_{FRET} = 6.9 × 10^{10} s^{-1}, Φ_{FRET} = 81.0%, k_{ISC} = 5.83 × 10^{9} s^{-1}, and τ_T = 147.9 μs. Different singlet oxygen ($^1O_2$) quantum yields (Φ_Δ = 75% and 70%) and triplet state quantum yields (Φ_T = 91% and 69%, respectively) were observed for complexes **Pt-1** and **Pt-4**.

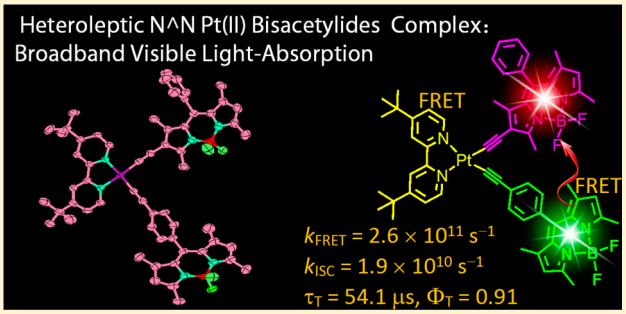

INTRODUCTION

Transition metal complexes, such as Pt(II) bisacetylide complexes, have attracted much attention owing to the applications in electroluminescence,[1] photocatalysis,[2] such as photocatalytic hydrogen (H_2) production,[3] photoredox catalytic organic reactions,[4] photovoltaics, and photoinduced charge separation,[5−10] nonlinear optics,[11−14] and more recently the triplet−triplet annihilation (TTA) upconversion.[15−22] However, conventional N^N Pt(II) acetylide complexes show weak absorption of visible light and short-lived triplet excited states (usually less than 10 μs).[23−34] These features are disadvantages for applications of these complexes as photosensitizers because the crucial photophysical processes concerning these applications are usually *intermolecular* energy or electron transfer. These *intermolecular* processes can be enhanced with the long-lived triplet excited state and abundance of the molecules at the triplet excited state; the latter is proportional to the visible light harvesting ability of the complexes.[35]

In order to address these challenges, visible light harvesting Pt(II) complexes have been reported, for example, with ligands derived from Bodipy[36] or perylenebisimide (PBI) chromophores.[37,38] On the other hand, it is important to control the vectorial energy transfer in these multichromophore complexes in order to efficiently funnel the photoexcitation energy.[39] However, complexes may show elusive photophysics, for example, short-lived intraligand triplet state (^{3}IL) was observed with PBI chromophore.[37,38,40] Recently, we prepared a series of visible light harvesting Pt(II) complexes with acetylide ligand based on coumarin[41] and Bodipy.[19,21,42,43] Generally these complexes show strong absorption of visible light (ε is up to 68 000 M^{-1} cm^{-1} in the range 500−600 nm), and the triplet state lifetime is as long as 128.4 μs.[18,35] These complexes were used as efficient triplet photosensitizers for TTA upconversion and photooxidation.[35]

Received: April 10, 2015
Published: July 31, 2015

DOI: 10.1021/acs.inorgchem.5b00822
Inorg. Chem. 2015, 54, 7803−7817

Scheme 1. Molecular Structure and Synthetic Process[a]

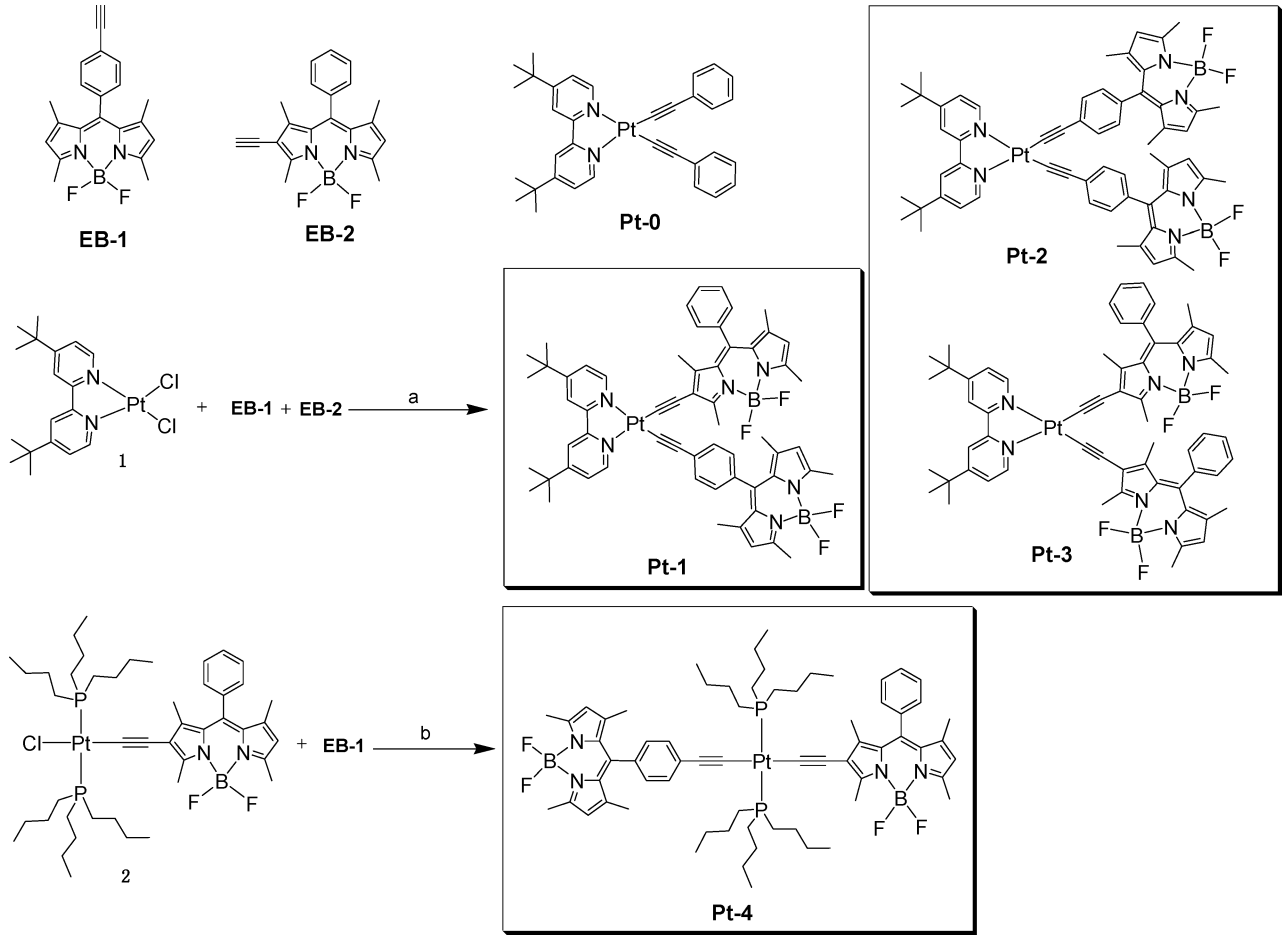

[a]The molecular structure of the ligands and reference complexes are also shown. (a) CuI, $(i\text{-Pr})_2NH$, dried CH_2Cl_2, argon, RT, 18 h, yield 28.8%. (b) Under Ar atmosphere, CuI, Et_2NH, distilled THF, ice bath, 1 h, yield 79.9%.

One of the remaining major drawbacks of these complexes is that the *single* chromophore motif of the molecular structures, i.e., there is only one kind of visible light absorbing ligand in the complex.[35] As a result, usually there is only *one* major absorption band in the visible spectral region for these complexes,[21] which is a clear disadvantage for harvesting the excitation energy of a *broad-band* light source, such as solar light. A multichromophore complex will address this challenge. Previously, Bodipy−porphyrin complexes were prepared.[44] However, porphyrin shows only moderate absorption in the visible region. Recently, we prepared Bodipy-containing bis(tributylphosphine) Pt(II) bisacetylide complexes with two different Bodipy ligands, and broad-band absorption in the visible spectral region was achieved.[43] However, it is clear that the molecular structural diversity needs to be extended and to investigate controlling the energy transfer in these multi-chromophore complexes with different alignment of the ligands.

Herein, we report a N^N Pt(II) bisacetylides complex (**Pt-1**, Scheme 1) containing two different Bodipy acetylide ligands, a rare molecular structural motif for N^N Pt(II) bisacetylide complexes.[23] Normally the two acetylide ligands in the N^N Pt(II) bis(acetylide) complex are the same. Using two different acetylide ligands for preparation of a N^N Pt(II) bisacetylides complex will give the product as a mixture (at least three products), which may make purification difficult. On the other hand, the trans bis(tributylphosphine) Pt(II) bisacetylides complex **Pt-4** was prepared as a reference complex in which the two different Bodipy ligands can be induced in a stepwise approach and the two ligands are aligned in different geometry as compared to that of **Pt-1** (Scheme 1). Both complexes **Pt-1** and **Pt-4** show broad-band absorption in the visible spectral region. The ligands are selected in such a way that the photoexcitation energy collected by the ligands was funneled onto one Bodipy ligand. The photophysical properties of the complexes were studied in detail with steady state and femto/nanosecond time-resolved transient absorption spectroscopies. Intramolecular singlet energy transfer was observed. Previously we have shown that the Bodipy chromophore can be used as an efficient photocatalytically active center for photocatalysis.[45−47] Thus, these results may become useful for designing efficient transition metal complex photosensitizers which show broad-band absorption of visible light and controllable FRET and ISC kinetics.

RESULTS AND DISCUSSION

Molecules Design and Synthesis. N^N Pt(II) bisacetylide complexes are usually prepared with the homoleptic acetylide ligands.[19,28,29,31,47−49] Using two different acetylide ligands will lead to a mixture of three major products; thus, this approach was rarely used for preparation of N^N Pt(II) bisacetylide complexes.[23] This situation is different from the

DOI: 10.1021/acs.inorgchem.5b00822
Inorg. Chem. 2015, 54, 7803−7817

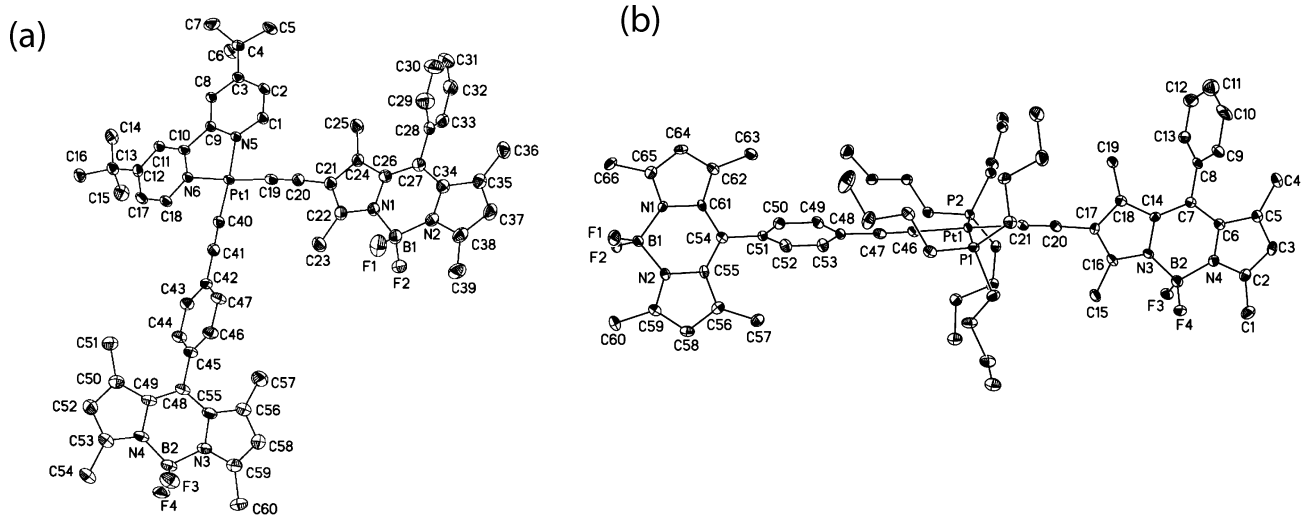

Figure 1. Perspective views of the single-crystal molecular structures of (a) **Pt-1** and (b) **Pt-4** with 50% thermal ellipsoid (hydrogen atoms were omitted for clarity).

trans bis(trialkylphosphine) Pt(II) bisacetylides complexes for which stepwise introduction of two different acetylide ligands is applicable. Previously, Suzuki et al. reported a N^N Pt(II) bisacetylides complex which contains two different acetylide ligands for study of photoinduced charge separation.[5] Following this method, herein we use two different acetylide ligands in the preparation of **Pt-1** (Scheme 1) for achieving broad-band visible light absorption and triplet state formation. To our satisfaction, the desired product was isolated from the reaction mixture with 28.8% yield (Scheme 1 and Experimental Section). The side products **Pt-2** and **Pt-3**, each containing homoleptic acetylide ligands, were isolated with yields of 16.1% and 12.7%, respectively. Reference complex **Pt-4** with the trans bis(tributylphosphine) coordination motif was also prepared for comparison (Scheme 1). Thus, the effects of the different alignment of the ligands on the photophysical properties of the complexes were studied. The femtosecond and nanosecond transient absorption spectroscopies indicated that the photophysics of **Pt-4** are drastically different from that of **Pt-1**.

Single-Crystal Molecular Structures. The single-crystal molecular structures of **Pt-1** and **Pt-4** were determined (Figure 1 and Table 1). For **Pt-1**, the two different linkages for the Bodipy ligands in the complexes were unambiguously confirmed (Figure 1). For the Pt(II) coordination center, a bond angle of N(5)−Pt−N(6) = 78.64° was observed. The angle of C(19)−Pt−C(40) is 87.95°. Previously for the similar complex with phenanthroline ligand, an N−Pt−N bond angle of 80.0° and a C−Pt−C bond angle of 89.8° was found.[29] The coordination geometry is close to a planar square geometry, but it is slightly distorted. The C−Pt distances are 1.955 and 1.945 Å, agreeing well with the reported Pt−C (acetylide) distance (1.943 and 1.950 Å).[29] The two N−Pt distances are 2.050 and 2.062 Å, respectively. The two Pt−C−C angles are 177.7° and 176.6°, respectively. Previously a Pt−C−C angle of 177.3° was found for a Pt(phen)[C≡C−(C_6H_4CHO)]$_2$ complex,[29] and the N−Pt distances for the same complex are 2.072 and 2.076 Å, respectively.[29] The distance of the B−B centers of the two Bodipy chromophore is 12.236 Å. It should be noted that the phenyl rings of the two Bodipy moieties take a perpendicular geometry toward the π core of Bodipy; thus, no π conjugation between the Pt(II) coordination center and the 8-phenyl Bodipy ligand is expected for **Pt-1**.

Table 1. Crystal Data Collection Parameters for Complex Pt-1 and Pt-4

parameter	Pt-1	Pt-4
sum formula	$C_{60}H_{60}B_2F_4N_6Pt$	$C_{67}H_{92}B_2Cl_2F_4N_4P_2Pt$
fw	1157.85	1379.00
temp. (K)	220	220
cryst syst	triclinic	triclinic
space group	*P*-1	*P*-1
a (Å)	11.5030 (3)	11.6142 (3)
α (deg)	72.083 (10)	106.3620 (10)
b (Å)	16.6531 (4)	16.3710 (4)
β (deg)	84.635 (2)	91.066 (2)
c (Å)	17.2268 (4)	18.6228 (4)
γ (deg)	84.876 (10)	103.144 (2)
vol. (Å^3)	3119.79 (13)	3295.48 (14)
Z	2	2
D_c (g·cm^{-3})	1.233	1.390
μ (mm^{-1})	2.299	2.312
F(000)	1172.0	1420.0
no. of reflns measured	18 081	17 365
no. of unique reflns (R_{int})	10 836 (0.0197)	11 403 (0.0404)
R_1[a]	0.0265	0.0374
ωR_2[b]	0.0709	0.0884
data completeness	0.986	0.984
goodness of fit	1.040	1.059

[a] $R_1 = \Sigma||F_o| - |F_c||/\Sigma|F_o|$. [b] $\omega R_2 = [\Sigma\omega(|F_o|^2 - |F_c|^2)/\Sigma\omega(F_o^2)^2]^{1/2}$; $\omega = 1/[\sigma^2(F_o^2) + (xP)^2 + yP]$, $P = (F_o^2 + 2F_c^2)/3$, where $x = 0.0415$ and $y = 1.8128$ for **Pt-1** and $x = 0.0307$ and $y = 0.0000$ for **Pt-4**.

The single-crystal molecular structure of **Pt-4** was also determined (Figure 1, Table 1, and Table S2, Supporting Information). The coordination geometry is drastically different from that of **Pt-1**. The C−Pt−C bond angle is 178.01° for **Pt-4**, slightly deviated from 180°. This result may be due to the less steric hindrance in **Pt-4**.[50] The two P−Pt−C angles in **Pt-4** are 93.74° and 87.20°, respectively. The B−B distance in **Pt-4** is 19.833 Å, much longer than that in **Pt-1** (12.236 Å). The distance between the two Bodipy ligands as well as the different alignment of the dipole moments in **Pt-1** and **Pt-4** may result in different photophysical processes, such as different FRET rate constants and energy transfer efficiency.

DOI: 10.1021/acs.inorgchem.5b00822
Inorg. Chem. 2015, 54, 7803−7817

Steady State UV−vis Absorption and Luminescence Spectra. The UV−vis absorption spectra of the complexes and ligands were studied (Figure 2). The ligands ethynylBodipy

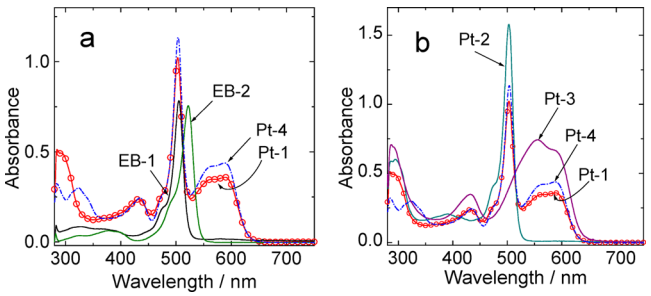

Figure 2. UV−vis absorption spectra of (a) **EB-1**, **EB-2**, **Pt-1**, and **Pt-4** and (b) **Pt-1**, **Pt-2**, **Pt-3**, and **Pt-4**. $c = 1.0 \times 10^{-5}$ M in toluene at 20 °C.

EB-1 and **EB-2** show absorption bands at 505 and 522 nm, respectively (Figure 2a). Upon coordination with Pt(II), **Pt-1** shows an intensive absorption at 503 nm and an absorption band at 588 nm. The absorption at the higher energy side is attributed to the coordinated **EB-1** ligand, whereas the absorption band at the lower energy side is due to the π-core-coordinated **EB-2** ligand.[19,21] Thus, the coordination profile of the two ligands exerts a significant effect on the absorption property. The excited state properties of **Pt-1** will be different from **Pt-4** because one of the compounds contains a diimine ligand while the other one does not.

These assignments of the absorption of **Pt-1** were supported by the UV−vis absorption of the reference complexes **Pt-2** and **Pt-3** (Figure 2b).[19,21] **Pt-2** shows a sharp intense absorption band at 503 nm, which is similar to the ligand of **EB-1**; thus, the π-conjugation framework of **EB-1** was not perturbed upon coordination. This result is due to the coordinate motif, i.e., the Pt(II) atom is not connected to the π-conjugation framework of **EB-1**. **Pt-3** show a broad absorption band in the range of 550−600 nm, which is different from that of **EB-2**. This result indicates that the π-conjugation framework of **EB-2** was significantly perturbed upon coordination. This result is due to the fact that the Pt(II) atom is connected to the π-conjugation framework of **EB-2**. Note that the absorption profile of **Pt-1** is superimposable to the sum of the absorption spectra of **Pt-2** and **Pt-3**, indicating that there no electronic interaction between the two different Bodipy ligands at the ground state. However, the absorption intensity of the two bands of **Pt-1** is about the one-half of that of **Pt-2** and **Pt-3**, respectively. This is reasonable since there is only one Bodipy ligand for each type of coordination motif in **Pt-1**, but there are two of the same ligands in **Pt-2** and **Pt-3**.

The UV−vis absorption of **Pt-4** is identical to that of **Pt-1**, especially in the visible spectral region. Since **Pt-4** is devoid of a MLCT state,[37,51] unlike that in **Pt-1**, we propose that the absorption of **Pt-4** in the visible region is mainly due to the ligand-localized absorption (IL), perturbed with Pt(II). Moreover, no significant MLCT absorption exists for **Pt-1** in the visible spectral region.

The UV−vis absorption spectra of the complexes in different solvents were studied (Figure 3). For **Pt-1**, the absorption band at 503 nm is almost independent to the solvent polarity, whereas the absorption band at 588 nm gives negative solvatochromism, i.e., the absorption shows a blue shift with

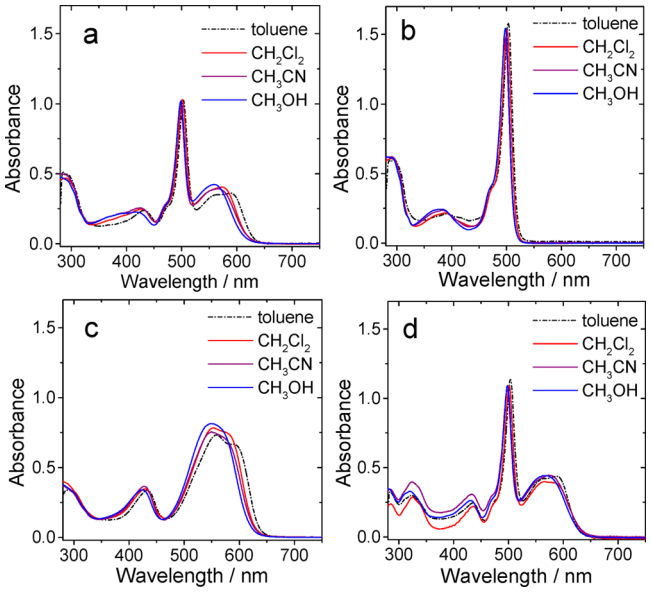

Figure 3. UV−vis absorption spectra of (a) **Pt-1**, (b) **Pt-2**, (c) **Pt-3**, and (d) **Pt-4** in different solvents. $c = 1.0 \times 10^{-5}$ M, 20 °C.

increasing solvent polarity. For example, the absorption maximum in toluene is 588 nm, but it is blue shifted to 558 nm in CH_3OH. This result indicates that the complex at the ground state is more stabilized by polar solvents than that of the S_1 state.[39] Similar results were observed for **Pt-3** and **Pt-4**.

The photoluminescence of the complexes was studied (Figure 4). **Pt-1** shows a major luminescence band at 518

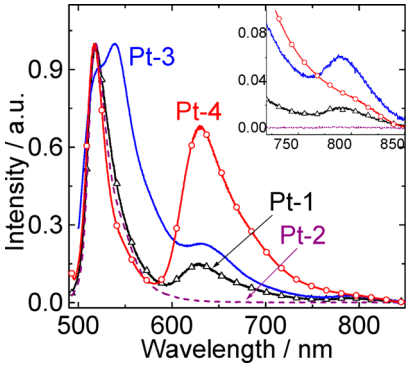

Figure 4. Normalized emission spectra of **Pt-1**, **Pt-2**, **Pt-3**, and **Pt-4** (λ_{ex} = 490 nm). $c = 1.0 \times 10^{-5}$ M in deaerated toluene at 20 °C.

nm, a minor band at 629 nm, and a very weak emission band at 792 nm. The small Stokes shift (15 nm, 575 cm^{-1}) and the short luminescence lifetime (1.9 ns) of the emission band at 518 nm are attributed to fluorescence of the coordinated 8-(4-ethynylphenyl)Bodipy ligand. On the other hand, the fluorescence emission band at 629 nm is due to the coordinated 2-ethynylBodipy ligand, which is supported by the similar emission profile of the reference complex **Pt-3**. The weak emission band of **Pt-1** at 792 nm is due to the phosphorescence of the coordinated 2-ethynyl Bodipy ligand. A similar phosphorescence emission band was observed for **Pt-3**. Emission band at 539 nm observed for **Pt-3** is probably due to the extremely small amount of free ligand **EB-2** (supported by the emission wavelength and luminescence lifetime; data are

DOI: 10.1021/acs.inorgchem.5b00822
Inorg. Chem. 2015, 54, 7803−7817

Table 2. Photophysical Properties of the Acetylide Ligands and Pt(II) Complexes

	λ_{abs} [a]	ε [b]	λ_{em} [a]	Φ_Δ (%) [c]	Φ_T (%) [e]	τ [g]	Φ_F (%) [i]
EB-1	505	7.66	520			2.4 ns	39.2
EB-2	522	7.65	539			5.9 ns	49.9
Pt-1	503/588	10.46/3.79	518/629/792	75.4 ± 1.5	91.3 ± 0.2	1.9 ns/0.3 ns/68.21 μs	0.46/0.49
Pt-2	503	15.87	518	37.1 ± 2.5 [d]	26.8 ± 0.5 [f]	134.7 ± 1.8 μs [h]	1.88
Pt-3	555	7.43	631/792	26.3 ± 1.5	49.2 ± 0.2	44.5 ± 1.5 μs [h]	0.3
Pt-4	504/587	11.37/4.38	517/631/783	70.1 ± 1.5	69.3 ± 0.2	147.9 ± 1.6 μs [h]	0.66/0.58

[a]In toluene (1.0×10^{-5} M), 20 °C, in nm. [b]Molar extinction coefficient at the absorption maxima. $\varepsilon = 10^4$ M^{-1} cm^{-1}. [c]Quantum yield of singlet oxygen ($^1O_2$), with methylene blue ($\Phi_\Delta = 0.57$ in CH_2Cl_2) as the standard, $\lambda_{ex} = 579$ nm. [d]With rose bengal ($\Phi_\Delta = 0.80$ in CH_3OH) as the standard, $\lambda_{ex} = 501$ nm. [e]Triplet states quantum yield, with methylene blue ($\Phi_T = 0.50$ in CH_3OH) as the standard, $\lambda_{ex} = 580$ nm. [f]With rose bengal ($\Phi_T = 0.90$ in CH_3OH) as the standard, $\lambda_{ex} = 514$ nm. [g]Luminescence lifetimes. [h]Triplet state lifetime; determined with nanosecond transient difference absorption spectroscopy; $\lambda_{ex} = 498$ nm, 1.0×10^{-5} M in deaerated toluene. [i]Fluorescence quantum yields. Bodipy ($\Phi_F = 72\%$ in THF) was used as standard. The deviations were determined by repetition of the measurement.

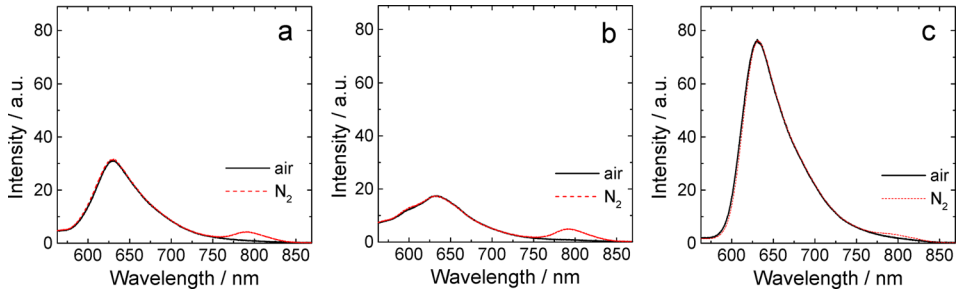

Figure 5. Photoluminescence spectra of (a) **Pt-1**, (b) **Pt-3**, and (c) **Pt-4**, under air and N_2 atmosphere with the same absorbance at the excitation wavelength $\lambda_{ex} = 555$ nm ($A = 0.74$, $c = 1.0 \times 10^{-5}$ M for **Pt-3**). The scale of the *y* axes were set the same in order to compare the emission intensity (in toluene at 20 °C).

not shown here), which is undetectable with thin layer chromatography (TLC).

The fluorescence emission of **Pt-1** does not necessarily indicate nonefficient ISC because the residual fluorescence is with very low quantum yield (0.5%, Table 2). Interestingly, **Pt-4** shows different luminescence as compared with that of **Pt-1**. Stronger fluorescence at 631 nm vs the fluorescence at 517 nm was observed. For **Pt-1**, the emission at 629 nm is much weaker.

The luminescence of the complexes with optically matched solutions are compared (Figure 5). **Pt-1** and **Pt-3** gave similar fluorescence/phosphorescence. However, for **Pt-4**, the fluorescence band is much stronger than the phosphorescence band. This result indicates that even with direct metalation of the π core of Bodipy, a different emission property may be observed with a different coordination motif. In other words, the emissive property of the complex is not only dependent on the heavy atom of the Pt(II) center but also may be dependent on the coordination motif of the Pt(II) center. The fluorescence intensity will be reciprocally related to the ISC, and the ISC is dependent on the ligands. Different ligands will induce different ISC efficiency.[23]

The emission spectra at 77 K were also measured (Figure 6). For **Pt-1**, the emission bands are slightly blue shifted as compared with that at RT. Furthermore, the phosphorescence band at 792 nm was intensified at 77 K (Figure 6a). For **Pt-4**, the emission band at 517 nm became much weaker at 77 K as compared with that of the 631 nm emission band. The phosphorescence band at 783 nm was intensified at 77 K (Figure 6b).

Luminescence Excitation Spectra: Intramolecular Resonance Energy Transfer. In order to study the intramolecular energy transfer (RET) in **Pt-1**, the luminescence

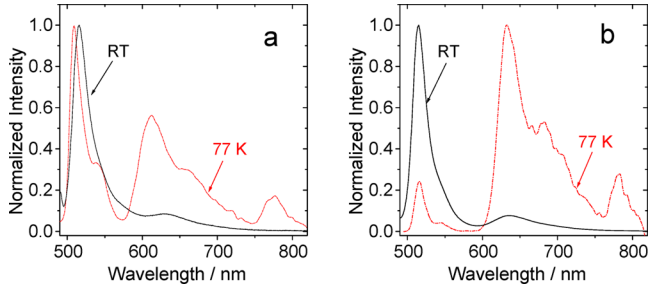

Figure 6. Normalized emission spectra of (a) **Pt-1** and (b) **Pt-4** in deaerated mixed solvent of methylcyclohexane/methyltetrahydrofuran/iodoethane (2:1:1, v/v) at room temperature (RT) and 77 K; $c = 1.0 \times 10^{-5}$ M, $\lambda_{ex} = 490$ nm.

excitation spectra of **Pt-1** were compared with those of that UV−vis absorption spectra (Figure 7a).[52] First, the emission of the coordinated 2-ethynyl Bodipy ligand at 680 nm in **Pt-1** was used as the monitoring wavelength in the measurement of the excitation spectrum. Two excitation bands were observed (Figure 7a). The broad one in the range 530−644 nm is the excitation of the coordinated 2-ethynyl Bodipy ligand. The excitation band at 503 nm is due to the coordinated 8-(4-ethynylphenyl)Bodipy ligand. This result indicates that there is singlet energy transfer from the coordinated 8-(4-ethynylphenyl)Bodipy ligand to the coordinated 2-ethynyl Bodipy ligand; otherwise, the band at 503 nm should not be observed in the excitation spectrum. The efficiency of this energy transfer is calculated as ca. 55%. The nonunity intramolecular RET may be due to the dipole moment orientation of the chromophores, nonoptimal spectral overlap, or photoinduced electron transfer.[52]

DOI: 10.1021/acs.inorgchem.5b00822
Inorg. Chem. 2015, 54, 7803−7817

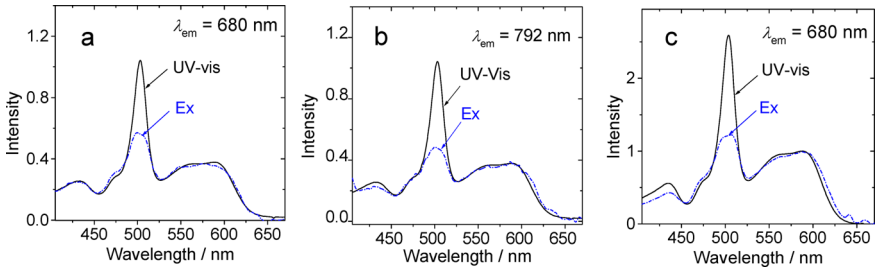

Figure 7. Normalized excitation and UV−vis absorption spectra of **Pt-1** determined with emission wavelength at (a) 680 and (b) 792 nm. (c) Normalized excitation and UV−vis absorption spectra of **Pt-4** (λ_{em} = 680 nm). c = 1.0 × 10^{-5} M in deaerated toluene at 20 °C.

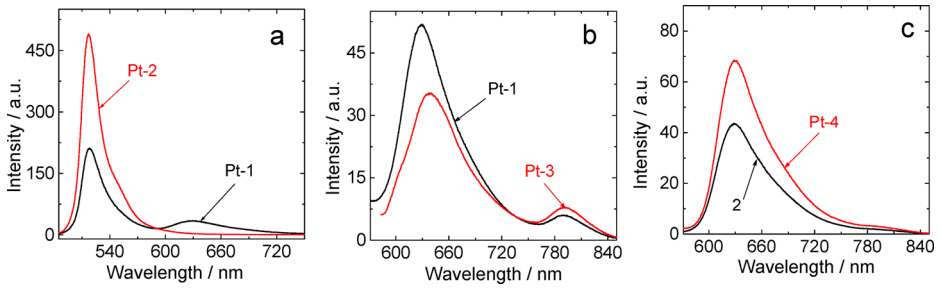

Figure 8. Comparison of the emission spectra of (a) **Pt-1** and **Pt-2** (λ_{ex} = 480 nm, A = 0.33), (b) **Pt-1** and **Pt-3** (λ_{ex} = 561 nm, A = 0.38), and (c) **2** and **Pt-4** (λ_{ex} = 555 nm, A = 0.38). Optically matched solutions were used in deaerated toluene at 20 °C.

The phosphorescence emission wavelength of **Pt-1** at 792 nm was also used as the monitoring wavelength for recording the excitation spectrum (Figure 7b). A similar excitation profile was observed. The excitation band at 501 nm indicates that the photoexcitation energy collected by the coordinated 8-(4-ethynylphenyl)Bodipy ligand can be transferred to the triplet excited state of **Pt-1**. The excitation spectrum of **Pt-4** with an emission wavelength at 680 was recorded and compared with the UV−vis absorption spectrum (Figure 7c). RET effect was confirmed; the energy transfer efficiency was calculated as ca. 50%.

It should be pointed out that the Bodipy ligands in **Pt-1** (and **Pt-4**) are attached on one Pt(II) atom; however, the two Bodipy ligands are not in π conjugation. These chromophores are electronically isolated from each other, which is supported by the UV−vis absorption motif of the complexes and reference compounds. Therefore, the above-mentioned photophysical processes can be described as FRET; otherwise, internal conversion is more appropriate.

Luminescence Quenching of the Energy Donor and Acceptor: Intramolecular Energy Transfer and Electron Transfer. In order to study the intramolecular singlet energy transfer (the 8-(4-ethynylphenyl)Bodipy moiety is the donor, while the 2-ethynylBodipy moiety is the acceptor), as well as the intramolecular electron transfer in **Pt-1**, the photoluminescence of **Pt-1** and **Pt-2** was compared with the reference compound solutions that show the same optical density at the excitation wavelength (480 nm, Figure 8a; optically matched solutions were used). The emission of the coordinated ligand was quenched in **Pt-1** to one-half of the intensity of **Pt-2** (optically matched solutions were used). Thus, intramolecular RET is probable in **Pt-1**, although electron transfer cannot be excluded.

In order to study the possible photoinduced electron transfer in **Pt-1**, the luminescence of the energy acceptor was compared with **Pt-1** (Figure 8b). With the same optical density at the excitation wavelength, the solutions of both **Pt-1** and **Pt-3** show similar phosphorescence intensity at 792 nm. Thus, the photoinduced electron transfer in **Pt-1** is not significant. The photoluminescence of a reference complex **2** (Pt(EB-$_2$){P-[$(CH_2)_3CH_3$]$_3$}$_2$Cl) (EB = ethynylBodipy, Scheme 1) was compared with that of **Pt-4** (Figure 8c). It was found that the emission intensity at 631 nm for **Pt-4** is stronger than that of complex **2**. Thus, no significant PET between the two Bodipy ligands is expected for **Pt-4**; otherwise, the fluorescence of the energy acceptor will be quenched.

The fluorescence of the ligands was also compared with that of the complexes (Figure 9). The strong fluorescence of **EB-1** was significantly quenched in **Pt-1**, which may be due to ISC or

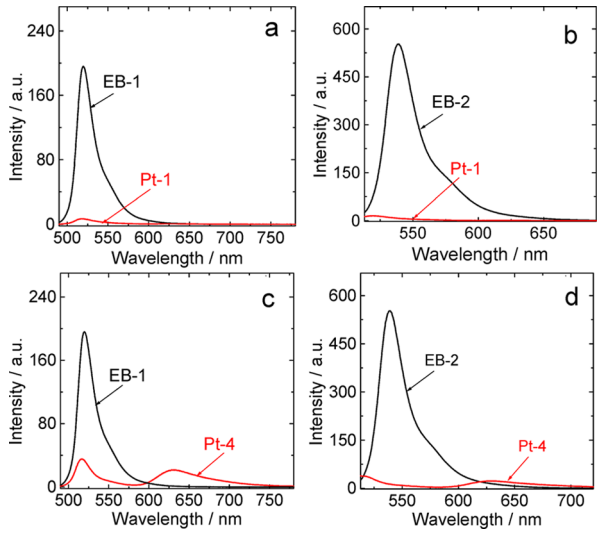

Figure 9. Emission spectra of (a) **Pt-1** and **EB-1** (λ_{ex} = 480 nm, A = 0.25), (b) **Pt-1** and **EB-2** (λ_{ex} = 511 nm, A = 0.54), (c) **Pt-4** and **EB-1** (λ_{ex} = 480 nm, A = 0.25), and (d) **Pt-4** and **EB-2** (λ_{ex} = 511 nm, A = 0.54); optically matched solutions were used. c = ca. 1.0 × 10^{-5} M in toluene at 20 °C.

DOI: 10.1021/acs.inorgchem.5b00822
Inorg. Chem. 2015, 54, 7803−7817

intramolecular RET (Figure 9a). PET may be responsible for the quenching of the fluorescence of the energy donor, but this case was excluded by studies in Figure 8b. The quenched fluorescence of the ligand **EB-2** (singlet energy acceptor) indicates an efficient ISC effect in **Pt-1** (Figure 9b). A similar quenching effect of the ligands in **Pt-4** was observed, which indicated RET and ISC effects (Figure 9c and 9d).

The photophysical properties of the compounds are compiled in Table 2. Note **Pt-1** shows broad-band absorption in the visible spectral region; the molecular absorption coefficients are very high (1.05×10^5 M^{-1} cm^{-1} at 503 nm and 3.79×10^4 M^{-1} cm^{-1} at 588 nm). Moreover, the singlet oxygen quantum yield (Φ_Δ) of **Pt-1** is as high as 75%. The quantum yield of triplet formation of **Pt-1** is $\Phi_T = 91\%$. These features make the complex **Pt-1** a promising photocatalyst for hydrogen (H_2) production or the photoredox catalytic organic reactions.[35]

Electrochemical Study: Cyclic Voltammetry. The electrochemical properties of the compounds were studied (Figure 10). For the reference complex **Pt-2**, an irreversible

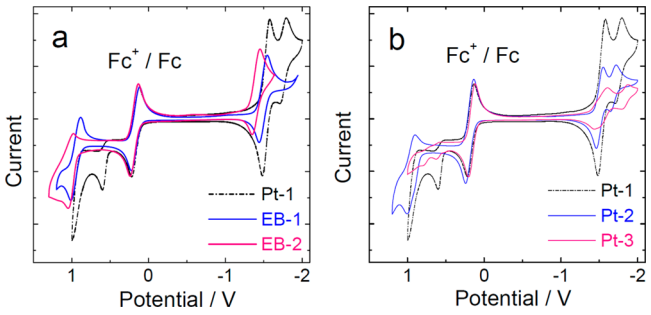

Figure 10. Cyclic voltammogram of (a) **EB-1**, **EB-2**, and **Pt-1** and (b) **Pt-1**, **Pt-2**, and **Pt-3**. Ferrocene (Fc) was used as internal reference ($E_{1/2}$ = +0.17 V, Fc^+/Fc). In deaerated CH_2Cl_2 solutions containing 1.0 mM photosensitizers and ferrocene (0.5 mM), 0.10 M Bu_4NPF_6 as supporting electrolyte, $Ag/AgNO_3$ reference electrode. Scan rate: 50 mV/s, 20 °C.

oxidation wave at ca. 1 V was observed. In the cathodic range, one reversible reduction wave at −1.46 V was observed and a pseudoreversible reduction wave was observed at −1.65 V. For **Pt-3**, an irreversible oxidation wave at +0.61 V was observed, which is attributed to the coordinated Bodipy ligands (via the 2 position of the Bodipy moiety). A similar result was observed for **Pt-1** at +0.61 V. This conclusion was supported by the Bodipy ligand coordinated to Pt(II) in a trans bis-(tributylphosphine) Pt(II) bisacetylide complex.[43] For **Pt-3**, two reversible reduction waves at −1.44 and −1.79 V were observed. We attribute the reduction potential of **Pt-1** at −1.71 V to reduction of the dbbpy ligand in **Pt-1**, whereas the reduction potential at −1.48 V is due to the Bodipy ligands.[27] Note the two different Bodipy ligands in **Pt-1** may show similar reduction potentials. Similar assignment was made for **Pt-2** and **Pt-3**.

The redox potentials of **Pt-1** were compared with the Bodipy ligands (Figure 10a). For **EB-1**, a pseudoreversible oxidation wave at +1.01 V was observed, together with a reduction wave at −1.44 V. For **EB-2**, slight anodically shifted oxidation (+1.05 V) and reduction waves (−1.35 V) were observed as compared with that of **EB-1**, indicating the electron deficiency feature of **EB-2** vs **EB-1**. In the cathodic region, the reduction potentials of **Pt-1** are different from the ligands. Furthermore, the oxidation wave of **Pt-1** is more cathodically shifted as compared with that of the ligands. The redox potentials of **Pt-1**, **Pt-2**, and **Pt-3** were compared in Figure 10b. The oxidation pattern of **Pt-1** is different from that of **Pt-2** and **Pt-3**.

The redox potentials of **Pt-1** and **Pt-4** were compared (Figure 11). It was found that the reduction and oxidation

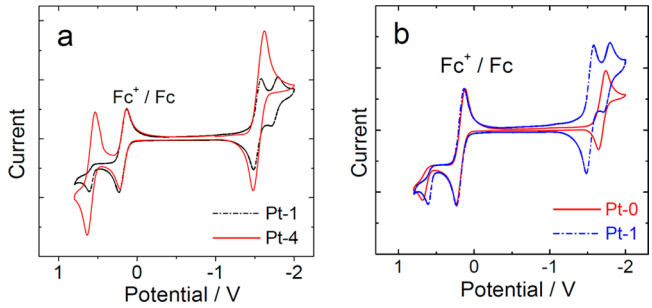

Figure 11. (a) Cyclic voltammograms of **Pt-1** and **Pt-4**. (b) Cyclic voltammograms of **Pt-0** and **Pt-1**. Ferrocene (Fc) was used as internal reference ($E_{1/2}$ = +0.17 V, Fc^+/Fc). In deaerated CH_2Cl_2 solutions containing 1.0 mM photosensitizers, 0.10 M Bu_4NPF_6 as supporting electrolyte, and $Ag/AgNO_3$ reference electrode. Scan rate: 50 mV/s, 20 °C.

bands of the two complexes are different. While **Pt-4** exhibits redox waves that are much more reversible, the actual potentials for one-electron oxidation and reduction do not differ significantly.

The intramolecular electron transfer in **Pt-1** was evaluated with the Gibbs free energy changes calculated with the Weller eqiation (eq 1 and eq 2).[53−55] ΔG_S is the static Coulombic energy, which is described by eq 2, where e = electronic charge, E_{OX} = half-wave potential for one-electron oxidation of the electron-donor unit (+0.61 V), E_{RED} = half-wave potential for one-electron reduction of the electron-acceptor unit (−1.48 V), E_{00} = energy level for the singlet excited state approximated with the fluorescence emission wavelength (629 nm, 1.97 eV), or the triplet excited state approximated with the phosphorescence emission wavelength (792 nm, 1.57 eV), ε_S = static dielectric constant of the solvent, R_{CC} = is the center-to-center separation distance determined by DFT optimization of the geometry (12.5 Å), R_D is the radius of the electron donor (5.23 Å), R_A is the radius of the electron acceptor (5.01 Å), ε_S is the static dielectric constant of the solvent used for the electrochemical studies, and ε_0 is the permittivity of free space. The solvents used in the calculation of free energy of the electron transfer are toluene (ε_S = 2.4), dichloromethane (ε_S = 8.9), and acetonitrile (ε_S = 37.5).

$$\Delta G_{CS} = e[E_{OX} - E_{RED}] - E_{00} + \Delta G_S \quad (1)$$

$$\Delta G_S = -\frac{e^2}{4\pi\varepsilon_S\varepsilon_0 R_{CC}} - \frac{e^2}{8\pi\varepsilon_0}\left(\frac{1}{R_D} + \frac{1}{R_A}\right)\left(\frac{1}{\varepsilon_{REF}} - \frac{1}{\varepsilon_S}\right) \quad (2)$$

The energies of the charge-separated states (E_{CS}) and the free energy change of the charge recombination process (ΔG_{CR}) were calculated with eqs 3 and 4.

The free energy changes are positive values, indicating that the photoinduced intramolecular electron transfer in **Pt-1** and **Pt-4** is thermodynamically prohibited.[53] This conclusion is in agreement with the spectra and the triplet state study of the complexes.

DOI: 10.1021/acs.inorgchem.5b00822
Inorg. Chem. 2015, 54, 7803−7817

Table 3. Redox Potentials of the Compounds[a]

compound	oxidation (V)	reduction (V)
EB-1	+1.01	−1.44
EB-2	+1.05	−1.35
Pt-0	+0.68	−1.64
Pt-1	+0.61	−1.48, −1.71
Pt-2	+1.01	−1.46, −1.65
Pt-3	+0.61, +0.79	−1.44, −1.79
Pt-4	+0.64	−1.46

[a]Cyclic voltammetry in Ar-saturated CH_2Cl_2 containing 1.0 mM photosensitizers, 0.10 M Bu_4NPF_6 supporting electrolyte, Pt electrode as the counter electrode, glassy carbon electrode as the working electrode, and $Ag/AgNO_3$ couple as the reference electrode. Ferrocene (Fc) was used as internal reference ($E_{1/2}$ = +0.17 V, Fc^+/Fc). Scan rate: 50 mV/s, 20 °C.

$$E_{CS} = e[E_{OX} - E_{RED}] + \Delta G_S \quad (3)$$

$$\Delta G_{CR} = -(\Delta G_{CS} + E_{00}) \quad (4)$$

Table 4. Driving Forces of Charge Separation (ΔG_{CS}), Static Coulombic Energy (ΔG_S), and Charge Recombination (ΔG_{CR}) Free Energy Values for Pt-1 and Pt-4

sample	solvent	ΔG_{CS} (eV)[a]	ΔG_{CS} (eV)[b]	ΔG_S (eV)	ΔG_{CR} (eV)
Pt-1	toluene	+0.46	+0.90	+0.38	−2.47
	CH_2Cl_2	−0.04	+0.40	−0.13	−1.96
	CH_3CN	−0.18	+0.25	−0.27	−1.82
Pt-4	toluene	+0.61	+1.10	+0.56	−2.66
	CH_2Cl_2	+0.03	+0.46	−0.08	−2.02
	CH_3CN	−0.21	+0.28	−0.26	−1.84

[a]Singlet excited state. [b]Triplet excited state.

Nanosecond Transient Absorption Spectroscopy. The triplet states of the complexes were studied with nanosecond transient absorption (TA) spectroscopy (Figure 12).[44,47,56−58] The nanosecond TA spectra of **Pt-1** were studied. Upon selective photoexcitation into the energy donor part (498 nm), a bleaching band at 560 nm was observed (Figure 12a). However, the bleaching band corresponding to the directly photoexcited energy donor did not appear. This result confirms the intramolecular triplet energy transfer in **Pt-1**, since our previous study confirmed that the triplet state can be produced with **Pt-2**.[19] The triplet state lifetime of **Pt-1** was determined as 54.1−56.6 μs. This lifetime is shorter than the lifetime of **Pt-2** (134.7 μs) but longer than **Pt-3** (44.5 μs). Normally the N^N Pt(II) bisacetylide complexes have a short triplet state lifetime, except a few complexes which contain pyrene,[59] Bodipy,[19] or naphthalimide ligands.[60]

Upon 582 nm nanosecond pulsed laser excitation, a bleaching band at 570 nm was observed for **Pt-1** (Figure 12c), which is similar to the results observed upon 498 nm photoexcitation. This bleaching band at 570 nm is due to depletion of the ground state of the coordinated 2-ethynylBodipy ligand. The TA band in the range of 300−500 and 650−850 nm is similar to that of **Pt-3**.[19] On the basis of these results, we propose that the triplet excited state of **Pt-1** is localized on the coordinated 2-ethynylBodipy ligand.[19,21] The coordinated 8-(4-ethynylphenyl)Bodipy ligand does not contribute to the T_1 triplet state of **Pt-1** because no bleaching band at ca. 500 nm was observed. Thus, intramolecular energy transfer occurs for **Pt-1**, so that the photoexcitation energy was funneled to one of the two coordinated ligands.

In order to prove the triplet state energy transfer in **Pt-1**, the *intermolecular* energy transfer between **Pt-2** (the energy donor) and **Pt-3** (the energy acceptor) was studied (with the mixture of the two complexes) as a mimic for the *intramolecular* triplet−triplet energy transfer (TTET) photophysical process in **Pt-1** (Figure 13).[61] With this approach, at least the relative energy level of the two coordinated ligands in **Pt-1** can be evaluated. Moreover, the kinetics of the *intramolecular* and *intermolecular* TTET can be compared. With increasing the **Pt-2**/**Pt-3** molar ratio, the decay of the transient of **Pt-2** became faster, with emerging of the transient absorption signal of **Pt-3** (Figure 13b−f).

The decay kinetics of the transient of the **Pt-2**/**Pt-3** mixture were monitored at two specific wavelengths (500 and 560 nm,

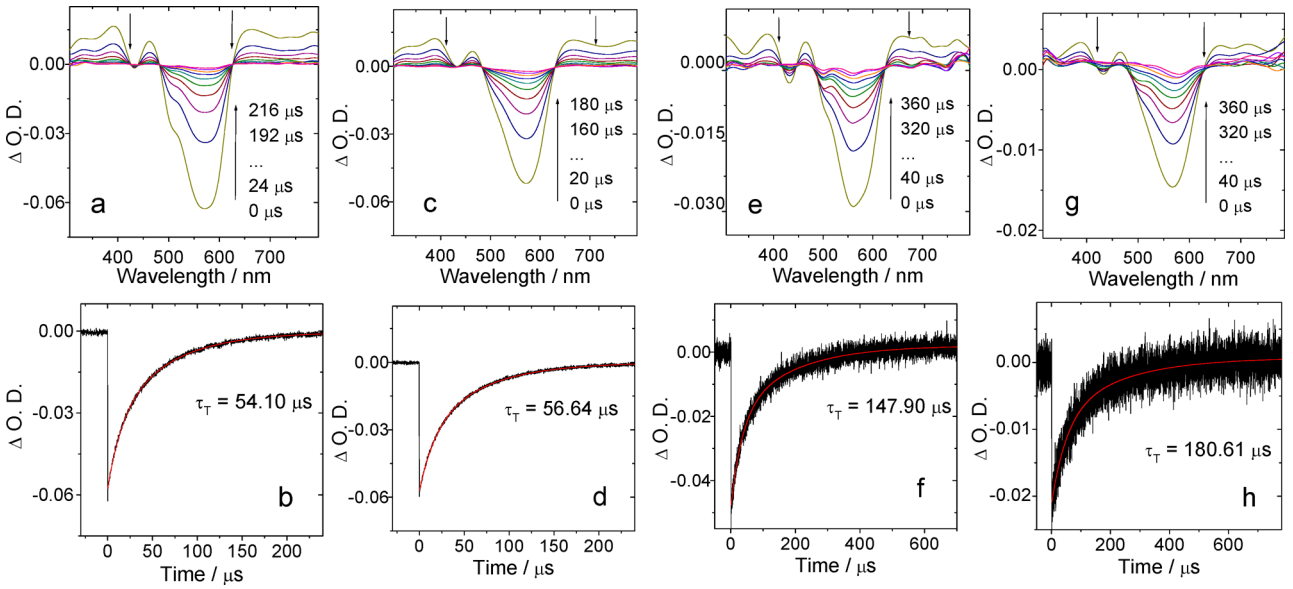

Figure 12. Nanosecond transient absorption spectra (a, c, e, and g) and decay trace at 560 nm (b, d, f, and h). (a and b) **Pt-1**, λ_{ex} = 498 nm, (c and d) **Pt-1**, λ_{ex} = 582 nm, (e and f) **Pt-4**, λ_{ex} = 498 nm, (g and h) **Pt-4**, λ_{ex} = 582 nm, c = 1.0 × 10^{-5} M, in deaerated toluene, 20 °C.

DOI: 10.1021/acs.inorgchem.5b00822
Inorg. Chem. 2015, 54, 7803−7817

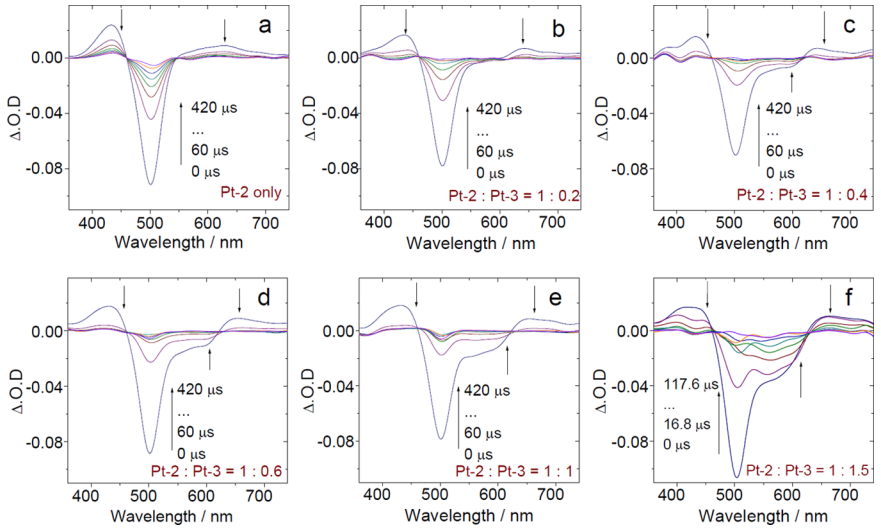

Figure 13. Nanosecond transient absorption spectra of the mixture of **Pt-2** and **Pt-3**. The concentration of **Pt-2** was fixed at 1.0×10^{-5} M, while the concentration of **Pt-3** was varied at (a) 0.0×10^{-5}, (b) 2.0×10^{-6}, (c) 4.0×10^{-6}, (d) 6.0×10^{-6}, (e) 1.0×10^{-5}, and (f) 1.5×10^{-5} M, λ_{ex} = 490 nm, in deaerated toluene, 20 °C.

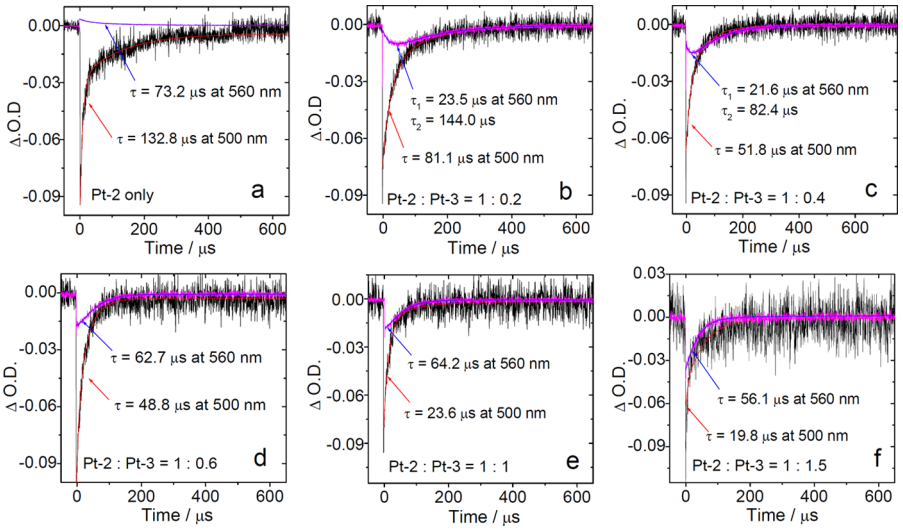

Figure 14. Decay traces of the mixture of **Pt-2** and **Pt-3** at 500 and 560 nm with increasing concentration of **Pt-3**. The concentration of **Pt-2** was fixed at 1.0×10^{-5} M, while the concentration of **Pt-3** was varied at (a) 0.0×10^{-5}, (b) 2.0×10^{-6}, (c) 4.0×10^{-6}, (d) 6.0×10^{-6}, (e) 1.0×10^{-5}, and (f) 1.5×10^{-5} M, λ_{ex} = 490 nm, in deaerated toluene at 20 °C.

Figure 14). With a **Pt-2**/**Pt-3** molar ratio of 1:0.2, the decay time of the transient at 500 nm is 81.1 μs, shorter than that of **Pt-2** alone (132.8 μs), which indicates triplet state quenching due to intermolecular TTET. At the same time, the development of the transient at 560 nm shows a biphasic character (Figure 14b), i.e., there is a increasing phase before 45 μs, thereafter the transient signal decays within ca. 350 μs. The increasing phase of the decay curve at 560 nm indicated the formation and accumulation of the triplet state of **Pt-3** via intermolecular TTET, whereas the decreasing phase after ca. 50 μs indicated the decay of the triplet excited state of **Pt-3**. Note the lifetime at 560 nm was decreased to 56.1 μs, which is very close to the lifetime of **Pt-3** alone (44.5 μs. Table 2).[19] With increasing the molar ratio of **Pt-2**/**Pt-3** (Figure 14b–f), the intermolecular TTET becomes faster. The energy transfer rates (k_{ET}) are 4.8×10^3, 1.2×10^4, 1.3×10^4, 3.5×10^4, and 4.3×10^4 s^{-1}, respectively ($k_{ET} = 1/\tau - 1/\tau_0$, τ_0 is the triplet state lifetime of the triplet energy donor in the absence of energy acceptor; τ is the triplet state lifetime of the triplet energy donor in the presence of energy acceptor). The bimolecular rate constant ($k_q = k_{sv}/\tau_0$) is 3.04×10^9 M^{-1} s^{-1}, which is comparable to a reported intermolecular triplet state energy transfer (7.04×10^9 M^{-1} s^{-1})[61] or an intra-assembly triplet state energy transfer (9.2×10^5 s^{-1}).[62]

Femtosecond Transient Absorption Spectroscopy. Ultrafast pump–probe experiments were performed for study of the FRET in **Pt-1** and **Pt-4**, as well as the ISC processes of the complexes (Figure 15). For ligands **EB-1** and **EB-2** as well as complexes **Pt-1**, **Pt-2**, **Pt-3**, and **Pt-4**, appropriate pump wavelengths were selected based on the steady-state UV–vis absorption spectroscopy. It is expected that FRET may occur for **Pt-1** and **Pt-4**, which contain two different kinds of ligands (**EB-1** and **EB-2**, with different S_1 state energy level, spectral overlap was observed). The ultrafast transient absorption spectra of **Pt-2** and **Pt-3** were studied (Supporting Information,

DOI: 10.1021/acs.inorgchem.5b00822
Inorg. Chem. 2015, 54, 7803–7817

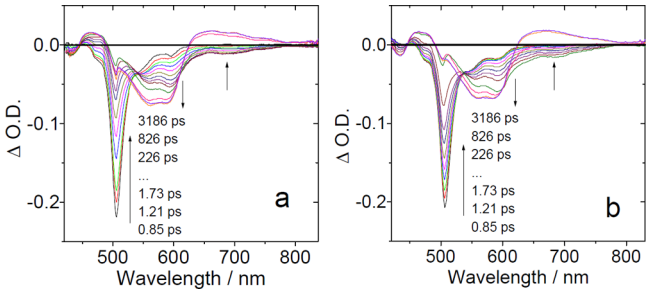

Figure 15. Femtosecond transient absorption spectra of **Pt-1** (a) and **Pt-4** (b) compounds at different time delays with 505 nm excitation. $c = 1.0 \times 10^{-5}$ M in deaerated toluene, 20 °C.

Figure S13) as references for interpretation of the photophysical properties of **Pt-1** and **Pt-4**.

Upon selective excitation into the singlet energy donor in **Pt-1** at 505 nm (the coordinated **EB-1** ligand), bleaching bands were observed at around 505 and 575 nm, where the coordinated ligands **EB-1** and **EB-2** give steady state absorption, respectively (Figure 15a). Moreover, the bleaching band at around 505 nm decreases, while the bleaching signal around 592 nm increases, simultaneously (Figure 16a). The

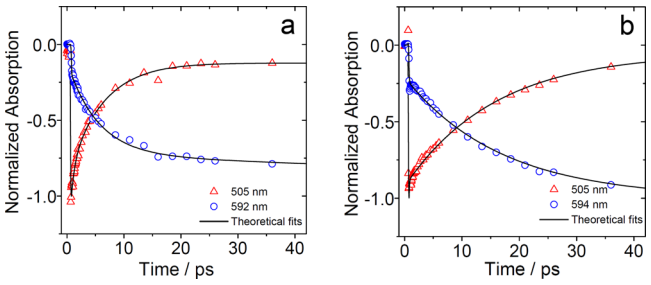

Figure 16. Decay traces of (a) **Pt-1** at 505 and 592 nm and (b) **Pt-4** at 505 and 594 nm. With 505 nm excitation. $c = 1.0 \times 10^{-5}$ M in deaerated toluene at 20 °C.

decay time of the bleaching signal of the coordinated ligand **EB-1** (505 nm) is about 3.9 ps, which is approximately equal to the rise time of the bleaching signal at 592 nm **Pt-1** (Figure 16a), i.e., the ground state bleaching of the coordinated **EB-2** ligand in **Pt-1**. This result unambiguously confirms the FRET process in **Pt-1** ($k_{FRET} = 2.6 \times 10^{11}$ s^{-1}, 3.9 ps). Direct comparison of the FRET with other N^N Pt(II) bisacetylides complexes is difficult because no N^N Pt(II) bisacetylides complexes containing two different visible light harvesting acetylide ligands with FRET were reported.[23] However, the kinetics of the FRET in **Pt-1** is comparable to the fast FRET in organic dyads, such as the Bodipy−azaBodipy triad (8.3 ps).[53] FRET with a kinetics of 2.5−8.7 ps was observed for Bodipy−porphyrazine conjugates.[63] Previously 2.2 ps of FRET was observed for diketopyrrolopyrrole (DPP)−Bodipy triad.[64]

On the other hand, excited state absorption (ESA) bands with a long decay time appeared at 425 and 650 nm after 52.1 ps time delay were observed for **Pt-1** (Figure 15a; Supporting Information, Figure S14a). These signals are attributed to the $T_1 \rightarrow T_n$ transition of the coordinated ligand **EB-2** based on a previous study with nanosecond transient absorption spectroscopy on the triplet excited state of the Bodipy-containing N^N Pt(II) bisacetylides complex **Pt-3**.[19] Thus, the ISC of the coordinated **EB-2** in **Pt-1** takes 52.1 ps ($k_{ISC} = 1.92 \times 10^{10}$ s^{-1}). The ISC in N^NPt(II) complexes is highly dependent on the chromophore. For example, an ultrafast ISC was found for a naphthalenediimide-containing Pt(II) complex (ISC takes 0.9 ps).[58] Previously a N^N Pt(II) bisacetylide complex containing ligand **EB-2** was studied with nanosecond transient absorption spectroscopy, but the ISC process was not investigated.[19] Bodipy-containing Pt(II) and Ir(III) complexes were also reported, with the Bodipy π core not being directly metalated; the inherent ISC of the Bodipy ligand was not studied.[36,56] In a bichromophoric Bodipy−benzoporphyrin platinum complex, the FRET from the Bodipy antenna to the Pt(II) coordination center had a rate constant of $k_{FRET} = 7.8 \times 10^{11}$ s^{-1} (1.3 ps).[44] Previously it was reported that the ISC of 2,6-diiodoBodipy takes 200 ps ($k_{ISC} = 5.0 \times 10^{9}$ s^{-1}).[65] The ultrafast FRET and ISC processes in **Pt-1** are beneficial for energy funneling because the other quenching channels may be inhibited.[66]

Similar results were observed for **Pt-4**, for which the bleaching band at 500 nm decreased and the ground state bleaching band at 590 nm intensified concurrently (Figures 15b and Figure 16b). These results give strong evidence of FRET in **Pt-4**, and the singlet energy transfer is from the coordinated ligand **EB-1** to the coordinated ligand **EB-2**. Interestingly, the FRET process takes 14.5 ps ($k_{FRET} = 6.9 \times 10^{10}$ s^{-1}) (Figure 16b), which is much slower as compared with that in **Pt-1** (3.9 ps, $k_{FRET} = 2.6 \times 10^{11}$ s^{-1}). The relatively slower FRET in **Pt-4** as compared with that of **Pt-1** may be due to the longer distance of the Bodipy ligands in **Pt-4** (boron−boron distance is 19.83 Å) than that in **Pt-1** (boron−boron distance is 12.24 Å).[67,68] After 171.5 ps time delay, ESA with a long time component appeared above 625 nm for **Pt-4**. These signals are attributed to $T_1 \rightarrow T_n$ transition of the coordinated ligand **EB-2** (Figures 15 and 16). Thus, the ISC in **Pt-4** (171.5 ps, $k_{ISC} = 5.83 \times 10^{9}$ s^{-1}) is slower than that of **Pt-1** (52.1 ps, $k_{ISC} = 1.92 \times 10^{10}$ s^{-1}) (Figure 15). Herein, we clearly show the significant impact of the different alignment of the ligands in the complex on the photophysical properties. The ISC kinetics of complexes **Pt-1** and **Pt-4** were compared by monitoring the decay trace at the ESA wavelengths. It is clear that **Pt-1** has a faster ISC than **Pt-4** (see Supporting Information, Figure S14).

It should be noted that the ISC of the trans bis(trialkyl)-phosphine Pt(II) bisacetylide complex may show substantially different kinetics, dependent on the chromophores. For example, an ISC of 5.4 ps was observed for N^N Pt(II) bisacetylide complexes containing pyrenylacetylide ligands.[69] On the other hand, a trans bis(trialkyl)phosphine Pt(II) bisacetylide complex with diketopyrrolopyrrole ligand has an ISC of 135 ps.[40]

Table 5. FRET and ISC Rate Constants of the Complexes Using Ultrafast Pump Probe Spectroscopy (in Toluene)

compound	FRET rate constants	ISC rate constants
Pt-1	2.6×10^{11} s^{-1}, 3.9 ps	1.92×10^{10} s^{-1} (52.1 ps)
Pt-2		9.89×10^{9} s^{-1} (101.1 ps)
Pt-3		4.23×10^{10} s^{-1} (23.6 ps)
Pt-4	6.9×10^{10} s^{-1}, 14.5 ps	5.83×10^{9} s^{-1} (171.5 ps)

We also studied the possibility of the backward energy transfer from the coordinated ligand **EB-1** to the **EB-2** in complexes **Pt-1** and **Pt-4** by performing another pump probe experiment with 590 nm excitation for **Pt-1** and **Pt-4**, at which the energy acceptor, i.e., the coordinated **EB-2** ligand, was selectively excited. There is single bleach signal at 590 nm, which corresponds to the ground state bleaching of ligand **EB-**

DOI: 10.1021/acs.inorgchem.5b00822
Inorg. Chem. 2015, 54, 7803−7817

2. No bleaching band at 500 nm was observed, indicating *upward* singlet energy transfer is impossible. Triplet state energy transfer to the coordinated ligand **EB-1** was also excluded; otherwise, ground state bleaching bands at 500 nm should be observed (Figure 12c).

In order to investigate the solvent effect on the energy transfer in **Pt-1** and **Pt-4**, the ultrafast transient absorption spectra were also studied with THF as solvent. Energy transfer rates are slightly different for both compounds in THF than that in toluene (Supporting Information, Figures S15 and S16). For example, the FRET rate of **Pt-1** decreases from 2.5×10^{11} (in toluene) to 2.2×10^{11} s^{-1} (in THF). On the other hand, the FRET rate constant of **Pt-4** increased from 15.0 (6.7×10^{10} s^{-1}, in toluene) to 9.7 ps (1.0×10^{11} s^{-1}, in THF). The variation of the transient dipole moment of the chromophores in **Pt-1** and **Pt-4** in solvents with different polarity may be responsible for the different FRET kinetics. It is known that the FRET is based on dipole−dipole interaction (Förster mechanism), and the FRET rate constants are dependent on the transient dipole moments of the energy donor and energy acceptor.[68]

No FRET process between the Bodipy ligands were expected for **Pt-2** and **Pt-3**, which contain the same types of ligands (**EB-1** or **EB-2**). The Ultrafast transient absorption spectra of **Pt-2** show a single bleach band at 505 nm (Supporting Information, Figure S13a). Furthermore, the positive signal (ESA) at 600 nm appears after about 101.1 ps time delay, which is attributed to $T_1 \rightarrow T_n$ transition absorption (Supporting Information, Figure S14b).[19] Thus, the ISC rate constant of **Pt-2** is $k_{ISC} = 9.89 \times 10^9$ s^{-1}. Transient absorption spectra of **Pt-3** show two bleaching signals at 560 and 600 nm, which are consistent with the steady state absorption spectrum. Interestingly, while the 600 nm bleaching signal is decreasing, the 560 nm bleaching signal increases concomitantly (Supporting Information, Figure S13b). The positive signal above 630 nm that can be attributed to the $T_1 \rightarrow T_n$ transition appears after 23.6 ps time delay; thus, k_{ISC} of **Pt-3** is 4.23×10^{10} s^{-1} (Supporting Information, Figure S14b).[19]

The ISC in **Pt-3** is much faster than that in **Pt-2**. This different ISC kinetics may be attributed to the different heavy atom effect in **Pt-2** and **Pt-3** (thus spin−orbit coupling, SOC) exerted by the different coordination profiles of the Pt(II) with the Bodipy acetylide ligands. Previously we proposed that direct connection of the Pt(II) atom with the π core of a chromophore will facilitate the ISC.[35] Importantly, the drastically different ISC in **Pt-2** and **Pt-3** indicated that the ISC of the coordinated **EB-1** ligand in **Pt-1** (and probably also in **Pt-4**) was overwhelmingly inhibited by the ultrafast FRET to the **EB-2** ligands, which is then followed by the ISC on the coordinated **EB-2** ligand.

The ultrafast pump probe spectroscopy of the ligands **EB-1** and **EB-2** was also studied. Ground state bleaching signal was observed at 505 and 525 nm in the transient absorption spectra of **EB-1** and **EB-2** compounds (see Supporting Information, Figure S19). There is an interesting oscillation with time delay in the bleach signals for **EB-1** and **EB-2** compounds. Note that we double-checked Bodipy compounds without a triple bond and did not see this oscillation occurring in time. This oscillation may be electron transfer between the Bodipy moiety and the triple bond. There is also a positive signal (excited state absorption) below 460 nm wavelength. This signal can be attributed to $S_1 \rightarrow S_n$ transition for these compounds. These bleach signals were fitted with a biexponential profile. Although one of the time components of **EB-1** and **EB-2** compounds is approximately equal (about 60 ps), the long-lived components are different from each other (~2000 and ~4500 ps, respectively). These times are in agreement with the fluorescence lifetimes of **EB-1** and **EB-2** as 2.4 and 5.9 ns, respectively (Table 2).

As mentioned above, femtosecond ultrafast transient absorption spectroscopies indicate the FRET in both **Pt-1** and **Pt-4**. Moreover, substantially different FRET and ISC kinetics were observed for **Pt-1** and **Pt-4**. We also show that the ISC kinetics of the Bodipy ligands with different coordination profiles (connection of Pt(II) with the π core or the meso phenyl moiety of the Bodipy chromophore) can vary up to 4-fold (**Pt-2** and **Pt-3**). These results are helpful for designing multichromophore Pt(II) complexes or molecular devices to show the predetermined photophysics, such as FRET and ISC.

DFT Calculations. The ground state geometry and the electronic excited states of **Pt-1** were studied with theoretical calculations (DFT method).[70−72] At the ground state, 2-ethynylBodipy has a coplanar geometry toward the Pt(II)−dbbpy coordination center. For the 8-(4-ethynylphenyl) Bodipy ligand, however, noncoplanar geometry was found. The Bodipy moiety in this ligand was separated from the Pt(II)−dbbpy coordination moiety by a phenyl ring. These DFT-optimized ground state structures are in agreement with the single-crystal molecular structure determinations.

The frontier molecular orbitals of **Pt-1** are presented in Figure 17. The molecular orbitals are confined on each of the two Bodipy ligands; there is no π conjugation between the two Bodipy units. This theoretical result is in agreement with the steady state UV−vis absorption. The T_1 state of **Pt-1** is featured as a mixed MLCT, LLCT, and IL transition, demonstrated by the H → L and H → L + 1 components of the transition. The T_1 and T_2 states are with the same components, and the state is mainly localized on the 2-ethynylBodipy ligand. The T_3 state is localized on the other Bodipy ligand. The T_4 state of **Pt-1** was identified as a state with mixed MLCT and LLCT feature, which are typical for the N^N Pt(II) bisacetylide complexes.[8,9]

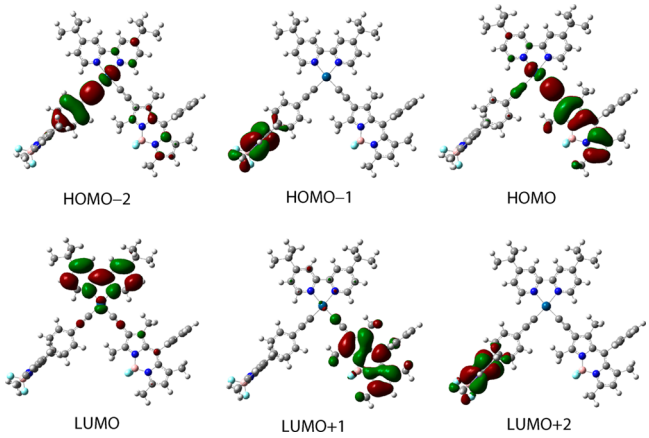

Figure 17. Electron density maps of the frontier molecular orbitals of **Pt-1**, calculated by DFT at the B3LYP/GENECP level with Gaussian 09W.

The spin density surfaces of complexes **Pt-1** and **Pt-4** were calculated (Figure 18). The spin density surfaces in both complexes are confined on the 2-ethynylated Bodipy ligand. Notably, the Pt(II) center contributes a little to the spin density surface; this is in agreement with the experimental results on the triplet state localization derived from nanosecond transient

DOI: 10.1021/acs.inorgchem.5b00822
Inorg. Chem. 2015, 54, 7803−7817

Table 6. Electronic Excitation Energies (eV) and Corresponding Oscillator Strengths (f), Main Configurations, and CI Coefficients of the Low-Lying Electronic Excited States of Complex Pt-1[a]

	electronic transition	energy[b]	f[c]	composition[d]	CI[e]	character
singlet	$S_0 \rightarrow S_1$	2.02 eV/614 nm	0.279	H → L	0. 691	LLCT
	$S_0 \rightarrow S_2$	2.32 eV/534 nm	0. 328	H → L + 1	0.672	ILCT
	$S_0 \rightarrow S_4$	2.46 eV/503 nm	0.212	H −2 → L	0.671	LLCT
				H − 2 → L + 1	0.136	LLCT
	$S_0 \rightarrow S_{11}$	2.95 eV/420 nm	0.614	H − 1 → L + 2	0.653	ILCT
triplet	$T_1 \rightarrow S_0$	1.43 eV/868 nm	0.000[f]	H → L	0.332	LLCT
				H → L + 1	0.584	ILCT
	$T_2 \rightarrow S_0$	1.54 eV/803 nm	0.000[f]	H → L	0.603	LLCT
				H → L + 1	0.304	ILCT
	$T_3 \rightarrow S_0$	1.61 eV/770 nm	0.000[f]	H − 1 → L + 2	0.707	ILCT
	$T_4 \rightarrow S_0$	1.92 eV/646 nm	0.000[f]	H − 2 → L	0.680	LLCT

[a]Calculated by TDDFT//B3LYP/GENECP, based on the DFT//B3LYP/GENECP-optimized ground state geometries. [b]Only the selected low-lying excited states are presented. [c]Oscillator strengths. [d]Only the main configurations are presented. [e]CI coefficients are in absolute values. [f]No spin−orbital coupling effect was considered; thus, the f values are zero.

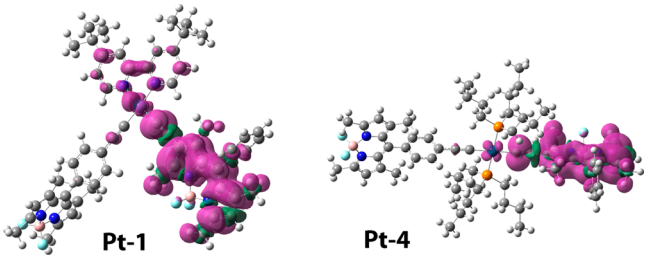

Figure 18. Spin density surfaces of **Pt-1** and **Pt-4** at the optimized triplet state geometry; calculated at B3LYP/LANL2DZ level with Gaussian 09W.

absorption spectroscopy (Figure 12). Furthermore, the 8-(4-ethynylphenyl)Bodipy ligand does not contribute to the spin density surface of complex **Pt-1**, which is also in agreement with the nanosecond transient absorption spectroscopy of **Pt-1**. Similar results were observed for **Pt-4**. The contribution of the Pt(II) atom to the triplet state in **Pt-4** is at less extent than that in **Pt-1**.

The photophysical properties of complex **Pt-1** are summarized in Scheme 2. The two Bodipy ligands were excited at different wavelengths. RET from the coordinated **EB-1** ligand to the coordinated **EB-2** ligand occurred after excitation into the **EB-1** moiety. Then ISC occurred; the coordinated **EB-2** moiety has a T_1 state energy level of 1.43 eV, lower than the coordinated **EB-1** ligand. Thus, the T_1 excited state of **Pt-1** will be localized on the coordinated **EB-2** ligand. This conclusion is supported by nanosecond transient absorption spectroscopy as well as spin density surface analysis based on the DFT calculation. We noted the energy level of the charge transfer state (2.47 and 1.82 eV in toluene and acetonitrile, respectively) has higher energy than the **EB-2** triplet state (1.43 eV); thus, the triplet excited state lifetime of **Pt-1** is independent of the solvent polarity (τ_T = 54.1 and 52.9 μs in toluene and acetonitrile, respectively). On the other hand, the CTS lies at lower energy than the singlet state of **EB-2**; thus, the fluorescence was quenched in acetonitrile as compared with that in toluene (Supporting Information, Figure S20).

Scheme 2. Simplified Jablonski Diagram Illustrating the Photophysical Processes Involved in Pt-1: (a) in Toluene and (b) in CH_3CN[a]

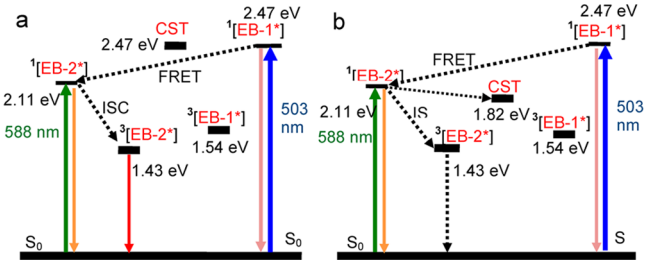

[a]The energy levels of the excited state are derived from the spectroscopic data and the electrochemical data. [**EB-1**] stands for the 8-(4-ethynylphenyl)Bodipy moiety, while [**EB-2**] stands for the 2-ethynyl Bodipy moiety in **Pt-1**.

CONCLUSIONS

In summary, a broad-band visible light absorbing dbbpy Pt(II) heteroleptic bisacetylides (dbbpy = 4,4′-di(*tert*-butyl)-2,2′-bipyridine) complex (**Pt-1**) was prepared with two different Bodipy acetylide ligands (**EB-1**, with acetylide on the meso phenyl position, and **EB-2**, with acetylide at the 2 position of the π core of Bodipy chromophore), a rarely studied molecular structural motif. Resonance energy transfer (RET) between the two different acetylide ligands is devised. A reference complex with the trans bis(tributylphosphine) Pt(II) bisacetylide geometry (**Pt-4**) and the heteroleptic acetylide ligands (**EB-1** and **EB-2**) was prepared for comparison of the photophysical properties. The photophysical properties of the complexes were studied with steady state UV−vis absorption and luminescence spectroscopies, femto- and nanosecond transient absorption spectroscopies, cyclic voltammetry, as well as DFT calculations. The two different Bodipy ligands in **Pt-1** and **Pt-4** constitute singlet/triplet energy donor/acceptor; as a result the harvested photoexcitation energy can be funneled to a confined ligand (coordinated **EB-2**). With different alignment for the two acetylide ligands, **Pt-1** and **Pt-4** show drastically different photophysical properties. The ultrafast intramolecular singlet energy transfer in **Pt-1** were confirmed by transient absorption spectroscopy (k_{FRET} = 2.6 × 10^{11} s^{-1}); the intersystem crossing rate constant (k_{ISC}) is 1.92 × 10^{10} s^{-1}, and the triplet state lifetime (τ_T) is 54.1 μs. Interestingly, the reference complex **Pt-4** shows different photophysical properties of k_{FRET} = 6.9 × 10^{10} s^{-1}, k_{ISC} = 5.83 × 10^9 s^{-1}, and τ_T = 147.9 μs. We also show that the ISC kinetics of the Bodipy ligands with different

DOI: 10.1021/acs.inorgchem.5b00822
Inorg. Chem. 2015, 54, 7803−7817

coordination profiles (with the Pt(II) atom directly linked to the π core of the Bodipy or not) can vary up to 4-fold (**Pt-2**, with acetylide on the meso phenyl moiety of Bodipy, k_{ISC} = 9.89×10^9 s^{-1}, and **Pt-3**, with acetylide linker at the 2 position of the π core of the Bodipy chromophore, k_{ISC} = 4.23×10^{10} s^{-1}). Singlet oxygen ($^1O_2$) quantum yield (Φ_Δ = 75% and 70%) and triplet state quantum yields (Φ_T = 0.91 and 0.69, respectively) were determined for complexes **Pt-1** and **Pt-4**. This information is useful for designing Pt(II) complexes showing broad-band visible light absorption, resonance energy transfer, and funneling of the excitation energy into a confined ligand, via efficient intersystem crossing.

EXPERIMENTAL SECTION

Materials. Solvents were dried or distilled before use. K_2PtCl_4 was purchased from Aladdin Chemical Co., Ltd. (P. R. China). Ligands **EB-1** and **EB-2**,[19] compounds **1** and **2**,[43,73] and complexes **Pt-2** and **Pt-3**[44] were prepared according to the reported procedures. **Pt-4** was prepared by modified literature methods.[5]

Analytical Measurements. NMR spectra were recorded by a Bruker 400 MHz spectrometer with $CDCl_3$ as the solvent and tetramethylsilane ($Si(CH_3)_4$) as the standard at 0.00 ppm. High-resolution mass spectra (HRMS) were determined in a TOF MALDI-HR MS system (UK). Elemental analyses (C, H, and N) were performed on a Perkin-Elmer model 240C elemental analyzer. Fluorescence spectra were measured on a RF5301 PC spectrofluorometer (Shimadzu, Japan), while the absorption spectra were recorded on a UV2550 UV−vis spectrophotometer (Shimadzu, Japan).

*Synthesis of **Pt-1**.* Under Ar atmosphere, Pt(dbbpy)Cl_2 (complex **1**, dbbpy = 4,4′-di(*tert*-butyl)-2,2′-bipyridine) (80.0 mg, 0.15 mmol), **EB-1** (52.0 mg, 0.15 mmol), and **EB-2** (52.0 mg, 0.15 mmol) were dissolved in dichloromethane (12 mL). After addition of diisopropylamine (0.6 mL) to the mixture via syringe, CuI (2.9 mg, 0.10 equiv) was added. Then the mixture was stirred at room temperature (RT) for 18 h. The solvents were removed under reduced pressure, and the solid was purified by column chromatography (silica gel; CH_2Cl_2:MeOH = 100:1, v/v). **Pt-1** was collected as a dark purple solid (50.4 mg, yield 28.8%). **Pt-2** (28.0 mg, yield 16.1%) and **Pt-3** (22.1 mg, yield 12.7%) were isolated as side products. For **Pt-1**, red crystals were grown by slow liquid diffusion of hexanes into a concentrated solution of **Pt-1** in CH_2Cl_2. Mp > 250 °C. ^1H NMR (400 MHz, $CDCl_3$): δ 9.71 (d, J = 4.0 Hz, 1H), 9.67 (d, J = 4.0 Hz, 1H), 7.96 (s, 2H), 7.63 (d, J = 4 Hz, 2H), 7.56 (d, J = 8.0 Hz, 2H), 7.48−7.45 (m, 3H), 7.31 (d, J = 4 Hz, 2H), 7.12 (d, J = 8.0 Hz, 2H), 5.98 (s, 2H), 5.93 (s, 1H), 2.83 (s, 3H), 2.56 (s, 6H), 2.55 (s, 3H), 1.60 (s, 6H), 1.56 (s, 3H), 1.45 (s, 18H), 1.36 (s, 3H). ^{13}C NMR (100 MHz): 163.6, 163.5, 160.0, 156.2, 156.1, 155.1, 153.4, 151.2, 151.1, 143.4, 142.5, 142.4, 141.5, 140.7, 135.4, 132.8, 131.6, 131.5, 131.3, 131.2, 129.1, 129.0, 128.7, 128.2, 127.3, 124.8, 124.6, 121.6, 121.0, 120.3, 118.8, 101.5, 93.3, 92.6, 88.5, 35.8, 31.9, 30.3, 29.7, 29.4, 22.7, 14.7, 14.6, 14.5, 14.2, 14.1, 14.0, 13.6. MALDI-HRMS: calcd ($[C_{66}H_{60}B_2F_4N_6Pt]^+$) m/z = 1157.4650, found m/z = 1157.4653. Anal. Calcd for $[C_{66}H_{60}B_2F_4N_6Pt]$: C, 62.24; H, 5.22; N, 7.26. Found: C, 62.29; H, 5.24; N, 7.24.

*Synthesis of **Pt-4**.* Under Ar atmosphere, compounds **EB-1** (21.0 mg, 0.06 mmol) and **2** (58.8 mg, 0.06 mmol) were dissolved in a mixed solvent of freshly distilled THF and diethylamine (16 mL, 1:1, v/v), and then the flask was put in an ice−water mixture for 15 min of cooling. After the reaction mixture was cooled, the flask was evacuated and backfilled with Ar 5 times. CuI (11.4 mg, 0.006 mmol) was added, and the mixture was stirred at RT for 45 min. Water (ca. 20 mL) was added, and the mixture was extracted with dichloromethane. The organic layer was dried over anhydrous sodium sulfate. After filtration, the solvent was removed under reduced pressure. The product was purified by column chromatography (silica, hexane, and dichloromethane, 2:3, v/v) to give **Pt-4** (62.0 mg, yield 79.9%) as a dark purple solid. Red crystals were obtained by slow liquid diffusion of methanol into a concentrated CH_2Cl_2 solution. Mp 205.2−206.1 °C. ^1H NMR (400 MHz, $CDCl_3$): δ 7.48−7.47 (m, 3H), 7.36 (s, 1H), 7.34 (s, 1H), 7.29−7.27 (m, 2H), 7.08 (s, 1H), 7.06 (s, 1H), 5.96 (s, 2H), 5.93 (s, 1H), 2.66 (s, 3H), 2.54 (s, 9H), 2.10−2.08 (m, 12H), 1.57−1.54 (m, 12H), 1.44−1.35 (m, 24H), 0.88 (t, J = 8 Hz, 18H). ^{13}C NMR (100 MHz): 158.7, 155.2, 153.6, 143.2, 142.3, 141.6, 140.8, 140.6, 135.4, 133.5, 131.3, 131.2, 131.1, 129.7, 129.0, 128.8, 128.1, 127.5, 122.3, 121.1, 120.4, 115.1, 110.3, 109.0, 99.7, 29.7, 26.4, 24.4, 24.4, 24.3, 24.1, 24.0, 23.8, 14.6, 14.3, 13.8, 13.2. MALDI-HRMS: calcd ($[C_{66}H_{90}B_2F_4N_4PtP_2]^+$) m/z = 1293.6411, found m/z = 1293.6420. Anal. Calcd for $[C_{66}H_{90}B_2F_4N_4PtP_2]$: C, 61.26; H, 7.01; N, 4.33. Found: C, 61.38; H, 7.02; N, 4.32.

Nanosecond Transient Absorption Spectroscopy. Nanosecond transient absorption spectra were recorded on a LP920 laser flash photolysis spectrometer (Edinburgh Instruments, Livingston, U.K.). The samples were purged with N_2 for 20 min before measurements, excited with a nanosecond pulse laser. The signal was digitized with a Tektronix TDS 3012B oscilloscope.

Femtosecond Transient Absorption Spectroscopy. The ultrafast wavelength-dependent pump probe spectroscopy measurements were performed using a Ti:Sapphire laser amplifier-optical parametric amplifier system (Spectra Physics, Spitfire Pro XP, TOPAS) and a commercial setup of ultrafast transient absorption spectrometer (Spectra Physics, Helios). Pulse duration was measured as 100 fs. Wavelengths of the pump beam were chosen according to the steady state absorption spectra of the studied compounds. White light continuum generated with a sapphire crystal was used as a probe beam.

Cyclic Voltammetry. Cyclic voltammetry was performed on a CHI610D electrochemical workstation (Shanghai, China). The measurements were performed under a 50 mV/s scan rate at room temperature. Tetrabutylammonium hexafluorophosphate ($Bu_4N[PF_6]$, 0.1 M) was used as the supporting electrolyte, while a glassy carbon electrode and a platinum electrode were the working electrode and counter electrode, respectively. Dichloromethane was used as the solvent with ferrocene (Fc) for the internal reference. The solution was purged with N_2 before measurement, and the N_2 gas flow was kept during the measurement.

DFT Calculations. Geometry optimization was calculated by the Becke-3-Lee−Yang−Parr (B3LYP) functional with a standard 6-31G(d) basis set for C, H, O, and N elements and the GENECP basis set for platinum, while the vertical excitation energy was calculated with the time-dependent DFT (TD-DFT) method based on the singlet ground state geometry. All calculations were performed with Gaussian 09W software (Gaussian, Inc.).[74] These methods were used because reasonable results can be obtained with these popular hybrids and basis set.

X-ray Crystallography. The intensity data of compounds **Pt-1** and **Pt-4** were collected on a Bruker SMART APEX CCD diffractometer equipped with a graphite-monochromated Mo Kα (λ = 0.71073 Å) radiation source; data were acquired using the SMART and SAINT programs.[75,76] The structures were solved by direct methods and refined on F^2 by full-matrix least-squares methods using the SHELXTL version 5.1 software.[77]

For crystal data of **Pt-1**, the non-hydrogen atoms were refined anisotropically. The hydrogen atoms within the ligand backbones were fixed geometrically at calculated distances and allowed to ride on the parent non-hydrogen atoms. The SQUEEZE subroutine in PLATON[78] was used with the cycle number being 1.

For crystal data of **Pt-4**, the non-hydrogen atoms were refined anisotropically. The hydrogen atoms within the ligand backbones and the CH_2Cl_2 molecule were fixed geometrically at calculated distances and allowed to ride on the parent non-hydrogen atoms. Crystal data and details of the data collection and structural refinements for **Pt-1** and **Pt-4** are summarized in Table 1. The selected bond lengths, bond distances, and angles of hydrogen bonds are presented in Tables S1 and S2, Supporting Information.

Tables of atomic coordinates, isotropic thermal parameters, and complete bond distances and angles have been deposited with the Cambridge Crystallographic Data Center. Copies of this information may be obtained free of charge, by quoting deposition numbers

DOI: 10.1021/acs.inorgchem.5b00822
Inorg. Chem. 2015, 54, 7803−7817

CCDC 1051812 (**Pt-1**) and 1051811 (**Pt-4**) from the Director, CCDC, 12 Union Road. Cambridge, CB2 1EZ, UK (fax +44-1223-336033; e-mail deposit@ccdc.cam.ac.uk; http://www.ccdc.cam.ac.uk).

■ ASSOCIATED CONTENT

Supporting Information

X-ray crystallographic data for **Pt-1** and **Pt-4** in CIF format, ^{1}H and ^{13}C NMR data, HRMS spectra, photophysical spectra, and DFT/TDDFT calculations of the complexes. The Supporting Information is available free of charge on the ACS Publications website at DOI: 10.1021/acs.inorgchem.5b00822.

■ AUTHOR INFORMATION

Corresponding Authors

*E-mail: zhaojzh@dlut.edu.cn.

*E-mail: hayvali@science.ankara.edu.tr.

Notes

The authors declare no competing financial interest.

■ ACKNOWLEDGMENTS

We thank the NSFC (20972024, 21273028, 21421005, and 21473020), the Royal Society (UK) and NSFC (China-UK Cost-Share Science Networks, 21011130154), the Ministry of Education (SRFDP-20120041130005), the Program for Changjiang Scholars and Innovative Research Team in University [IRT_13R06], the Fundamental Research Funds for the Central Universities (DUT14ZD226), and Dalian University of Technology (DUT2013TB07) for financial support.

■ REFERENCES

(1) (a) Chan, S.-C.; Chan, M. C. W.; Wang, Y.; Che, C.-M.; Cheung, K.-K.; Zhu, N. *Chem. - Eur. J.* **2001**, *7*, 4180−4190. (b) Langdon-Jones, E. E.; Hallett, A. J.; Routledge, J. D.; Crole, D. A.; Ward, B. D.; Platts, J. A.; Pope, S. J. A. *Inorg. Chem.* **2013**, *52*, 448−456. (c) Li, B.; Wen, H.-M.; Wang, J.-Y.; Shi, L.-X.; Chen, Z.-N. *Inorg. Chem.* **2013**, *52*, 12511−12520. (d) Zhang, L.-Y.; Xu, L.-J.; Zhang, X.; Wang, J.-Y.; Li, J.; Chen, Z.-N. *Inorg. Chem.* **2013**, *52*, 5167−5175.

(2) Mori, K.; Watanabe, K.; Fuku, K.; Yamashita, H. *Chem.—Eur. J.* **2012**, *18*, 415−418.

(3) Wang, X.; Goeb, S.; Ji, Z.; Pogulaichenko, N. A.; Castellano, F. N. *Inorg. Chem.* **2011**, *50*, 705−707.

(4) Feng, K.; Zhang, R.-Y.; Wu, L.-Z.; Tu, B.; Peng, M.-L.; Zhang, L.-P.; Zhao, D.; Tung, C.-H. *J. Am. Chem. Soc.* **2006**, *128*, 14685−14690.

(5) Suzuki, S.; Sugimura, R.; Kozaki, M.; Keyaki, K.; Nozaki, K.; Ikeda, N.; Akiyama, K.; Okada, K. *J. Am. Chem. Soc.* **2009**, *131*, 10374−10375.

(6) Lai, S.-W.; Chen, Y.; Kwok, W.-M.; Zhao, X.-J.; To, W.-P.; Fu, W.-F.; Che, C.-M. *Chem.—Asian J.* **2010**, *5*, 60−65.

(7) Lee, S.-H.; Chan, C. T.-L.; Wong, K. M.-C.; Lam, W. H.; Kwok, W.-M.; Yam, V. W.-W. *J. Am. Chem. Soc.* **2014**, *136*, 10041−10052.

(8) McGarrah, J. E.; Kim, Y.-J.; Hissler, M.; Eisenberg, R. *Inorg. Chem.* **2001**, *40*, 4510−4511.

(9) Chakraborty, S.; Wadas, T. J.; Hester, H.; Flaschenreim, C.; Schmehl, R.; Eisenberg, R. *Inorg. Chem.* **2005**, *44*, 6284−6293.

(10) Hua, F.; Kinayyigit, S.; Rachford, A. A.; Shikhova, E. A.; Goeb, S.; Cable, J. R.; Adams, C. J.; Kirschbaum, K.; Pinkerton, A. A.; Castellano, F. N. *Inorg. Chem.* **2007**, *46*, 8771−8783.

(11) Liu, R.; Azenkeng, A.; Zhou, D.; Li, Y.; Glusac, K. D.; Sun, W. *J. Phys. Chem. A* **2013**, *117*, 1907−1917.

(12) Liu, R.; Azenkeng, A.; Li, Y.; Sun, W. *Dalton Trans.* **2012**, *41*, 12353−12357.

(13) Guo, F.; Sun, W.; Liu, Y.; Schanze, K. *Inorg. Chem.* **2005**, *44*, 4055−4065.

(14) Yang, Z.-D.; Feng, J.-K.; Ren, A.-M. *Inorg. Chem.* **2008**, *47*, 10841−10850.

(15) Borisov, S. M.; Saf, R.; Fischer, R.; Klimant, I. *Inorg. Chem.* **2013**, *52*, 1206−1216.

(16) Du, P.; Eisenberg, R. *Chem. Sci.* **2010**, *1*, 502−506.

(17) Zhao, J.; Ji, S.; Guo, H. *RSC Adv.* **2011**, *1*, 937−950.

(18) Zhao, J.; Ji, S.; Wu, W.; Wu, W.; Guo, H.; Sun, J.; Sun, H.; Liu, Y.; Li, Q.; Huang, L. *RSC Adv.* **2012**, *2*, 1712−1728.

(19) Wu, W.; Liu, L.; Cui, X.; Zhang, C.; Zhao, J. *Dalton Trans.* **2013**, *42*, 14374−14379.

(20) Guo, H.; Li, Q.; Ma, L.; Zhao, J. *J. Mater. Chem.* **2012**, *22*, 15757−15768.

(21) Wu, W.; Zhao, J.; Guo, H.; Sun, J.; Ji, S.; Wang, Z. *Chem.—Eur. J.* **2012**, *18*, 1961−1968.

(22) Ji, S.; Wu, W.; Zhao, J.; Guo, H.; Wu, W. *Eur. J. Inorg. Chem.* **2012**, *2012*, 3183−3190.

(23) Williams, J. A. G. *Top. Curr. Chem.* **2007**, *281*, 205−268.

(24) Castellano, F. N.; Pomestchenko, I. E.; Shikhova, E.; Hua, F.; Muro, M. L.; Rajapakse, N. *Coord. Chem. Rev.* **2006**, *250*, 1819−1828.

(25) Wong, W.-Y.; Ho, C.-L. *Coord. Chem. Rev.* **2006**, *250*, 2627−2690.

(26) Ma, D.-L.; Ma, V. P.-Y.; Chan, D. S.-H.; Leung, K.-H.; He, H.-Z.; Leung, C.-H. *Coord. Chem. Rev.* **2012**, *256*, 3087−3113.

(27) Hissler, M.; Connick, W. B.; Geiger, D. K.; McGarrah, J. E.; Lipa, D.; Lachicotte, R. J.; Eisenberg, R. *Inorg. Chem.* **2000**, *39*, 447−457.

(28) Hua, F.; Kinayyigit, S.; Cable, J. R.; Castellano, F. N. *Inorg. Chem.* **2005**, *44*, 471−473.

(29) Wadas, T. J.; Lachicotte, R. J.; Eisenberg, R. *Inorg. Chem.* **2003**, *42*, 3772−3778.

(30) Yang, Q.-Z.; Wu, L.-Z.; Wu, Z.-X.; Zhang, L.-P.; Tung, C.-H. *Inorg. Chem.* **2002**, *41*, 5653−5655.

(31) Whittle, C. E.; Weinstein, J. A.; George, M. W.; Schanze, K. S. *Inorg. Chem.* **2001**, *40*, 4053−4062.

(32) Adams, C. J.; Fey, N.; Harrison, Z. A.; Sazanovich, I. V.; Towrie, M.; Weinstein, J. A. *Inorg. Chem.* **2008**, *47*, 8242−8257.

(33) Sazanovich, I. V.; Alamiry, M. A. H.; Meijer, A. J. H. M.; Towrie, M.; Davies, E. S.; Bennett, R. D.; Weinstein, J. A. *Pure Appl. Chem.* **2013**, *85*, 1331−1348.

(34) Glusac, K.; Köse, M. E.; Jiang, H.; Schanze, K. S. *J. Phys. Chem. B* **2007**, *111*, 929−940.

(35) Zhao, J.; Wu, W.; Sun, J.; Guo, S. *Chem. Soc. Rev.* **2013**, *42*, 5323−5351.

(36) Lazarides, T.; McCormick, T. M.; Wilson, K. C.; Lee, S.; McCamant, D. W.; Eisenberg, R. *J. Am. Chem. Soc.* **2011**, *133*, 350−364.

(37) Rachford, A. A.; Goeb, S.; Castellano, F. N. *J. Am. Chem. Soc.* **2008**, *130*, 2766−2767.

(38) Prusakova, V.; McCusker, C. E.; Castellano, F. N. *Inorg. Chem.* **2012**, *51*, 8589−8598.

(39) Sabatin, i. R. P.; Zheng, B.; Fu, W.-F.; Mark, D. J.; Mark, M. F.; Hillenbrand, E. A.; Eisenberg, R.; McCamant, D. W. *J. Phys. Chem. A* **2014**, *118*, 10663−10672.

(40) Goswami, S.; Winkel, R. W.; Alarousu, E.; Ghiviriga, I.; Mohammedqq, O. F.; Schanze, K. S. *J. Phys. Chem. A* **2014**, *118*, 11735−11743.

(41) Sun, H.; Guo, H.; Wu, W.; Liu, X.; Zhao, J. *Dalton Trans.* **2011**, *40*, 7834−7841.

(42) Wu, W.; Zhao, J.; Sun, J.; Huang, L.; Yi, X. *J. Mater. Chem. C* **2013**, *1*, 705−716.

(43) (a) Jia, H.; Kucukoz, B.; Xing, Y.; Majumdar, P.; Zhang, C.; Karatay, A.; Yaglioglu, G.; Elmali, A.; Zhao, J.; Hayvali, M. *J. Mater. Chem. C* **2014**, *2*, 9720−9736. (b) Yang, W.; Karatay, A.; Zhao, J.; Song, J.; Zhao, L.; Xing, Y.; Zhang, C.; He, C.; Yaglioglu, H. G.; Hayvali, M.; Elmali, A.; Küçüköz, B. *Inorg. Chem.* 2015, 10.1021/acs.inorgchem.5b01107

(44) Whited, M. T.; Djurovich, P. I.; Roberts, S. T.; Durrell, A. C.; Schlenker, C. W.; Bradforth, S. E.; Thompson, M. E. *J. Am. Chem. Soc.* **2011**, *133*, 88−96.

(45) Huang, L.; Cui, X.; Therrien, B.; Zhao, J. *Chem.—Eur. J.* **2013**, *19*, 17472−17482.

DOI: 10.1021/acs.inorgchem.5b00822
Inorg. Chem. 2015, 54, 7803−7817

(46) Huang, L.; Zhao, J. *RSC Adv.* **2013**, *3*, 23377−23388.
(47) Guo, S.; Zhang, H.; Huang, L.; Guo, Z.; Xiong, G.; Zhao, J. *Chem. Commun.* **2013**, *49*, 8689−8691.
(48) Rachford, A. A.; Goeb, S.; Ziessel, R.; Castellano, F. N. *Inorg. Chem.* **2008**, *47*, 4348−4355.
(49) McGarrah, J. E.; Eisenberg, R. *Inorg. Chem.* **2003**, *42*, 4355−4365.
(50) Chan, C. K. M.; Tao, C.-H.; Li, K.-F.; Wong, K. M.-C.; Zhu, N.; Cheah, K.-W.; Yam, V. W.-W. *Dalton Trans.* **2011**, *40*, 10670−10685.
(51) Chan, C. K. M.; Tao, C.-H.; Tam, H.-L.; Zhu, N.; Yam, V. W.-W.; Cheah, K.-W. *Inorg. Chem.* **2009**, *48*, 2855−2864.
(52) Kostereli, Z.; Ozdemir, T.; Buyukcakir, O.; Akkaya, E. U. *Org. Lett.* **2012**, *14*, 3636−3639.
(53) El-Khouly, M. E.; Amin, A. N.; Zandler, M. E.; Fukuzumi, S.; D'Souza, F. *Chem.—Eur. J.* **2012**, *18*, 5239−5247.
(54) Ziessel, R.; Allen, B. D.; Rewinska, D. B.; Harriman, A. *Chem.—Eur. J.* **2009**, *15*, 7382−7393.
(55) Hankache, J.; Wenger, O. S. *Chem.—Eur. J.* **2012**, *18*, 6443−6447.
(56) Rachford, A. A.; Ziessel, R.; Bura, T.; Retailleau, P.; Castellano, F. N. *Inorg. Chem.* **2010**, *49*, 3730−3736.
(57) Yarnell, J. E.; Deaton, J. C.; McCusker, C. E.; Castellano, F. N. *Inorg. Chem.* **2011**, *50*, 7820−7830.
(58) Sazanovich, I. V.; Alamiry, M. A. H.; Best, J.; Bennett, R. D.; Bouganov, O. V.; Davies, E. S.; Grivin, V. P.; Meijer, A. J. H. M.; Plyusnin, V. F.; Ronayne, K. L.; Shelton, A. H.; Tikhomirov, S. A.; Towrie, M.; Weinstein, J. A. *Inorg. Chem.* **2008**, *47*, 10432−10445.
(59) Pomestchenko, I. E.; Luman, C. R.; Hissler, M.; Ziessel, R.; Castellano, F. N. *Inorg. Chem.* **2003**, *42*, 1394−1396.
(60) Guo, H.; Muro-Small, M. L.; Ji, S.; Zhao, J.; Castellano, F. N. *Inorg. Chem.* **2010**, *49*, 6802−6804.
(61) El-Khouly, M. E.; Fukuzumi, S. *J. Porphyrins Phthalocyanines* **2011**, *15*, 111−117.
(62) Feng, K.; Yu, M.-L.; Wang, S.-M.; Wang, G.-X.; Tung, C.-H.; Wu, L.-Z. *ChemPhysChem* **2013**, *14*, 198−203.
(63) Engelhardt, V.; Kuhri, S.; Fleischhauer, J.; Garcia-Iglesias, M.; Gonzalez-Rodriguez, D.; Bottari, G.; Torres, T.; Guldi, D. M.; Faust, R. *Chem. Sci.* **2013**, *4*, 3888−3893.
(64) Harriman, A.; Alamiry, M. A. H.; Hagon, J. P.; Hablot, D.; Ziessel, R. *Angew. Chem., Int. Ed.* **2013**, *52*, 6611−6615.
(65) Sabatini, R. P.; McCormick, T. M.; Lazarides, T.; Wilson, K. C.; Eisenberg, R.; McCamant, D. W. *J. Phys. Chem. Lett.* **2011**, *2*, 223−227.
(66) Ziessel, R.; Harriman, A. *Chem. Commun.* **2011**, *47*, 611−631.
(67) Lakowicz, J. R. *Principles of Fluorescence Spectroscopy*, 2nd Ed.; Kluwer Academic: New York, 1999.
(68) Turro, N. J.; Scaiano, J. C.; Ramamurthy, V. *Principles of Molecular Photochemistry: An Introduction*; University Science Books: Sausalito, CA, 2008.
(69) Danilov, E. O.; Pomestchenko, I. E.; Kinayyigit, S.; Gentili, P. L.; Hissler, M.; Ziessel, R.; Castellano, F. N. *J. Phys. Chem. A* **2005**, *109*, 2465−2471.
(70) Adamo, C.; Jacquemin, D. *Chem. Soc. Rev.* **2013**, *42*, 845−856.
(71) Li, Z.; Ren, A.; Guo, J.; Yang, T.; Goddard, J. D.; Feng, J. *J. Phys. Chem. A* **2008**, *112*, 9796−9800.
(72) Zhao, G.-J.; Han, K.-L.; Stang, P. J. *J. Chem. Theory Comput.* **2009**, *5*, 1955−1958.
(73) Wong, W.-Y.; Harvey, P. D. *Macromol. Rapid Commun.* **2010**, *31*, 671−713.
(74) Frisch, M. J.; Trucks, G. W.; Schlege, 1. H. B.; Scuseria, G. E.; Robb, M. A.; Cheeseman, J. R.; Scalman, i. G.; Barone, V.; Mennucci, B.; Petersson, G. A.; Nakatsuji, H.; Caricato, M.; Li, X.; Hratchian, H. P.; Izmaylov, A. F.; Bloino, J.; Zheng, G.; Sonnenberg, J. L.; Hada, M.; Ehara, M.; Toyota, K.; Fukuda, R.; Hasegawa, J.; Ishida, M.; Nakajima, T.; Honda, Y.; Kitao, O.; Nakai, H.; Vreven, T.; Montgomery, J. A. J.; Peralta, J. E.; Ogliaro, F.; Bearpark, M.; Heyd, J. J.; Brothers, E.; Kudin, K. N.; Staroverov, V. N.; Kobayashi, R.; Normand, J.; Raghavachari, K.; Rendell, A.; Burant, J. C.; Iyengar, S. S.; Tomasi, J.; Cossi, M.; Rega, N.; Millam, M. J.; Klene, M.; Knox, J. E.; Cross, J. B.; Bakken, V.; Adamo, C.; Jaramillo, J.; Gomperts, R.; Stratmann, R. E.; Yazyev, O.; Austin, A. J.; Cammi, R.; Pomelli, C.; Ochterski, J. W.; Martin, R. L.; Morokuma, K.; Zakrzewski, V. G.; Voth, G. A.; Salvador, P.; Dannenberg, J. J.; Dapprich, S.; Daniels, A. D.; Farkas, O.; Foresman, J. B.; Ortiz, J. V.; Cioslowski, J.; Fox, D. J. *Gaussian 09*; Gaussian, Inc.: Wallingford, CT, 2009.
(75) *SMART Data collection software*, version 5.629; Bruker AXS Inc.: Madison, WI, 2003.
(76) *SAINT Data reduction software*, version 6.45; Bruker AXS Inc.: Madison, WI, 2003.
(77) Sheldrick, G. M. *SHELXS-97: Program for Crystal Structure Solution*; University of Göttingen: Göttingen, Germany, 1997.
(78) Spek, A. L. *J. Appl. Crystallogr.* **2003**, *36*, 7−13.

DOI: 10.1021/acs.inorgchem.5b00822
Inorg. Chem. 2015, 54, 7803−7817